Inorganic Chemistry Communications 158 (2023) 111446

Contents lists available at ScienceDirect

Inorganic Chemistry Communications

journal homepage: www.elsevier.com/locate/inoche

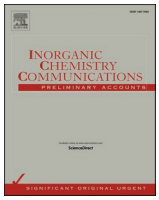

Metal-organic framework-based composites for energy, catalytic, and environmental applications: A critical review

K.A.U. Madhushani [a,b], A.A.P.R. Perera [a,b], Jasvinder kaur [c], Anuj Kumar [d,*], Ram K. Gupta [a,b,*]

[a] Department of Chemistry, Pittsburg State University, Pittsburg, KS 66762, United States
[b] National Institute for Materials Advancement, Pittsburg State University, Pittsburg, KS 66762, United States
[c] Department of chemistry, School of Sciences, IFTM University, Moradabad 244102, Uttar Pradesh, India
[d] Nano-Technology Research Laboratory, Department of Chemistry, GLA University, Mathura 281406, Uttar Pradesh, India

ARTICLE INFO

Keywords:
Metal-organic framework
CO_2 conversion
Catalytic properties
Energy density
Power density

ABSTRACT

Metal-organic framework (MOF)-based composites have the inherent morphological features of MOF, including controllable, uniform pores, a large surface area, a clearly defined crystal structure, and so on. Depending on the metals and ligands used in MOF and the kinds of functional groups added to MOF-based compounds, these composites can be used for a wide range of reactions, such as hydroxylation, CO reduction, CO_2 conversion, CO_2 adsorption, separation, cycloaddition, etc. In that scenario, several properties like weak catalytic activities, lower cyclic stability, and poor electrochemical performances limit the industrial-scale uses of those compounds. This leads to more attention among industrial and academic researchers to explore more ways to overcome the drawbacks of MOF-based materials. Considering their morphological and structural characteristics, these composites are mostly used for heterogeneous catalytic reactions. The aim of this review is to highlight the fundamental concepts of MOFs, encompassing their structural and morphological characteristics, alongside approaches for their conversion into composites. Additionally, this study emphasizes the recent advancements in heterogeneous catalytic performance and the use of MOF-based composites in catalytic, electrical, and optical applications. The subsequent section delves into an examination of the future problems and prospects associated with MOF-based composites. This review would help new readers grasp MOFs so they can enjoy their catalytic performances.

1. Introduction

With the increase in the global population, the demand for non-renewable energy sources (ex: fossil fuels) used in day-to-day activities is increasing at an alarming rate. The overconsumption of these resources brings numerous threatening effects on living beings and the environment. Due to these circumstances, most researchers have paid their attention to finding alternative energy sources as a solution to overcome this energy crisis. Discovering an eco-friendly, sustainable, low-cost, facile synthesized energy source that can replace fossil fuels, is quite a challenge [1].As a result of tremendous studies, Metal-organic frameworks (MOFs) have been introduced since 1995 [2]. As an introduction to this material, the nature of the MOF compound and the chemistry behind this structure are briefly discussed here. MOFs are familiarized as a form of long-range ordered crystalline porous materials, prepared from metal clusters or metals by organic ligands that are considered as their building block. Mostly, transitional metals/ cations from d-block (Ti^{4+}, Zr^{4+}, V^{3+}, Cr^{3+}, Fe^{3+}, Mn^{2}, Ni^{2}, Cu^{2}, Zn^{2}, Cd^{2+})/some other s-block (Mg^{2+})/p-block (Al^{3+}, Ga^{3+}) and few from the lanthanide/actinide series are used as metals while nitrogen or oxygen-containing donors act as linkers interacting with the metal ions. In MOF structure, metal ions/ dimers are represented as nodes resulting in forming complex arrangements from trimer to octal nuclear with hydroxy/ oxide anions [3]. Characteristically, MOFs have capable of achieving a high specific surface area of over 6000 m^2/g resulting from their high porosity which facilitates up to 90 % of free space. With the study of coordination chemistry behind the metal-ligands bond interaction and functionalization of organic groups, it is quite difficult to find an endpoint in this route of research based on MOF materials. This is because the properties and structure of the MOF can be altered by changing both the types of metals used in the synthesis and the nature of the organic linkers [4].

* Corresponding authors.
E-mail addresses: anuj.kumar@gla.ac.in (A. Kumar), ramguptamsu@gmail.com (R.K. Gupta).

https://doi.org/10.1016/j.inoche.2023.111446
Received 28 July 2023; Received in revised form 2 September 2023; Accepted 14 September 2023
Available online 21 September 2023

Considering the chemistry behind MOF, organic linkers having multitopic and rigid ligand molecules such as amines, bi-/ tri-/ tetra-topic carboxylates, and rarely sulfonates, and phosphonates are used to interact with organometallic nodes. As an example of monotropic carboxylates acting as bridging linkers, the synthesis of the manganese/ magnesium format of MOF can be introduced. These anionic linkages can control the charge of the cationic nodes. Aromatic or olefinic compounds are responsible for forming the backbone of the MOF, ultimately creating a highly porous crystalline network with greater stiffness and stability. Although most MOFs consist of one type of metal ion and linker, in some cases combinations of different types of metal ligands can be observed. However, the differences in linkers and metals used in MOFs, lead to diversity in structure and properties [3].

As a step forward in past studies on MOFs, MOF-based composites were investigated with the purpose of increasing the structural, electrical, catalytic, magnetic, and optical properties of an individual MOF. To date, various types of functional materials including carbon, quantum dots, metals, metal oxides, sulfides, phosphides, polymers, silica, etc. are incorporated into MOF to modify their properties **(**Fig. 1**)**. The effects of those materials on the MOF after synthesizing the composites are discussed in detail in the next section. In brief, the composites gain more properties due to the synergistic effects, and modification of the combined properties of MOF and guest material. In the fabrication of composites, the materials incorporated into the MOF are determined by the application in which they are used [1].Their incredible structural features and associated functional properties lead to carry out various discoveries and widen the fields of application in storage, catalytic, separation, etc. [5].Although these composites have many applications, this review mainly focuses on recent progress in the energy, catalysis, and environmental contributions of MOF-based composites. In addition, some other significant uses of these materials are briefly reviewed.

2. Characteristics of MOFs and their composites

2.1. Structural and physico-chemical properties of MOFs

Over the 18th century, the structural development of MOF began with the discovery of Prussian blue and Cu $[C(C_6H_4CN)_4]$ as CP and porous CP, respectively. In 1999, Yagi and his team invented MOF-5 which has a stable porous structure from Zn_4O clusters and dicarboxylate bonds [6]. As a result of this extensive research, modified version of MOFs has come up as ultra-porous (e.g., MIL-101), ultra-stable (e.g., UiO-66), and flexible (e.g., MIL-88). It has been reported that current research on these materials tends to explore the more novel findings of multivariate/ heterarchical MOFs (HT-MOF) with a wide variety and hierarchical MOFs (HR-MOF) having well-regulated designs. In HT-MOF, the elementary units are randomly organized in the framework while HR-MOF shows a sequence arrangement. However, both structures are linked to hierarchically maintained sequences within the system providing better macroscopic and molecular properties (Fig. 2**a**). Considering the structural evolution of MOF, initially prepared MOF using metal and ligands were developed into MOF crystallites, then self-assembled this structure as secondary and tertiary schemes respectively. Further discoveries have reached an extra modified quaternary superstructure that indicates the success of massive efforts in this field. At that time, molecular-level aggregation was the dominant focus in the development of MOFs. Thus, the latest innovation in MOF is based on the artificial technique used to introduce hierarchy into the secondary MOF structure [7].

Due to the structural tunability of MOFs, three different types of hierarchies of MOFs such as hierarchical (HR) porosity, HR architecture, and HR composition are introduced(Fig. 2**b**).When the building units are linked or mechanically designed using the templates, pores can be formed in the MOF [7].The presence of different pore sizes, such as micro-, meso-, and macroscopically with in the single frame of HR

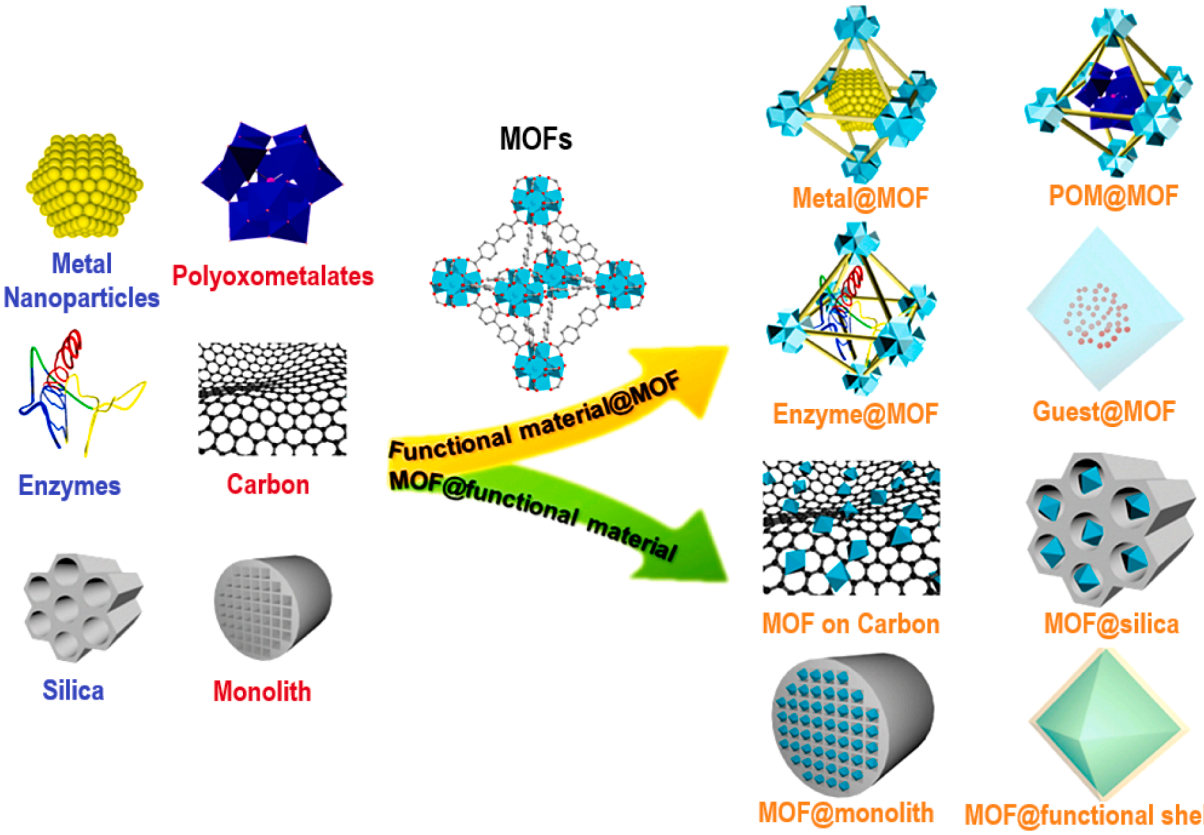

Fig. 1. Fabrication of various types of MOF composite by composing functional materials. Adapted with permission [5], Copyright (2019), Matter.

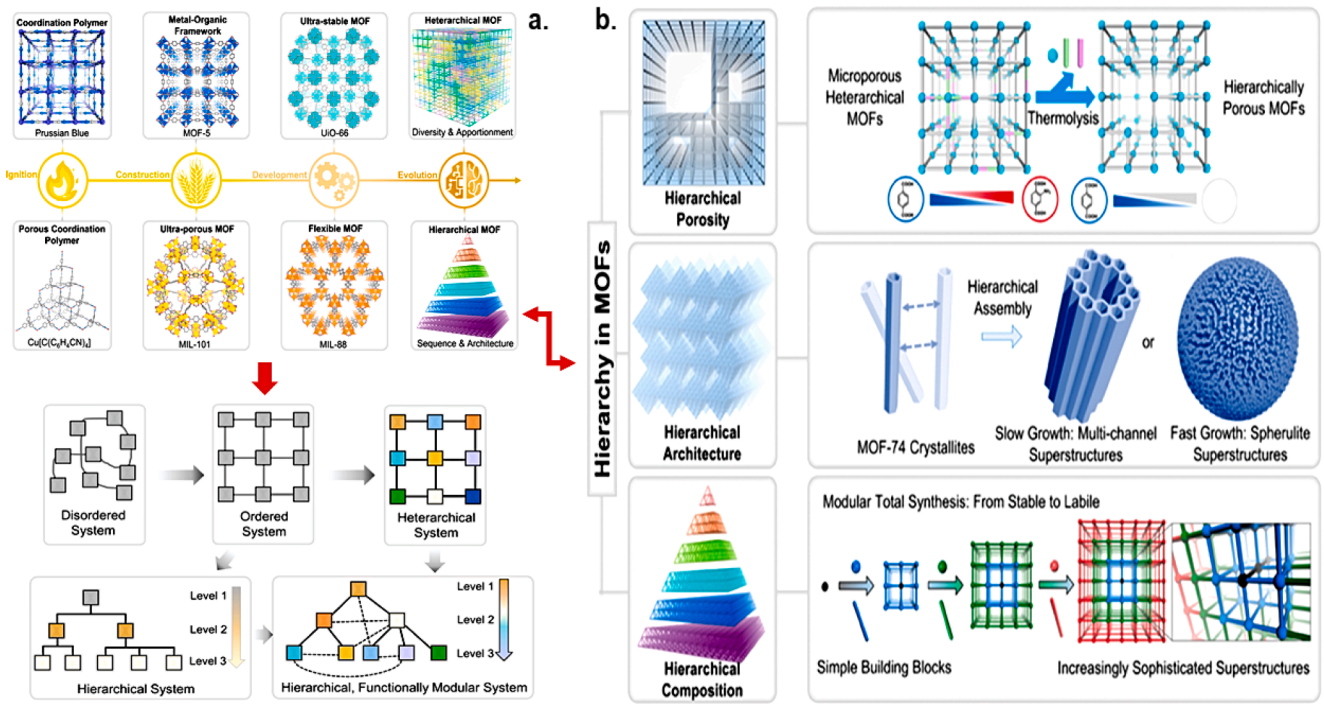

Fig. 2. Progress in MOF development from coordination polymer to hierarchical MOF. Adapted with permission [7], Copyright (2020), ACS Central Science.

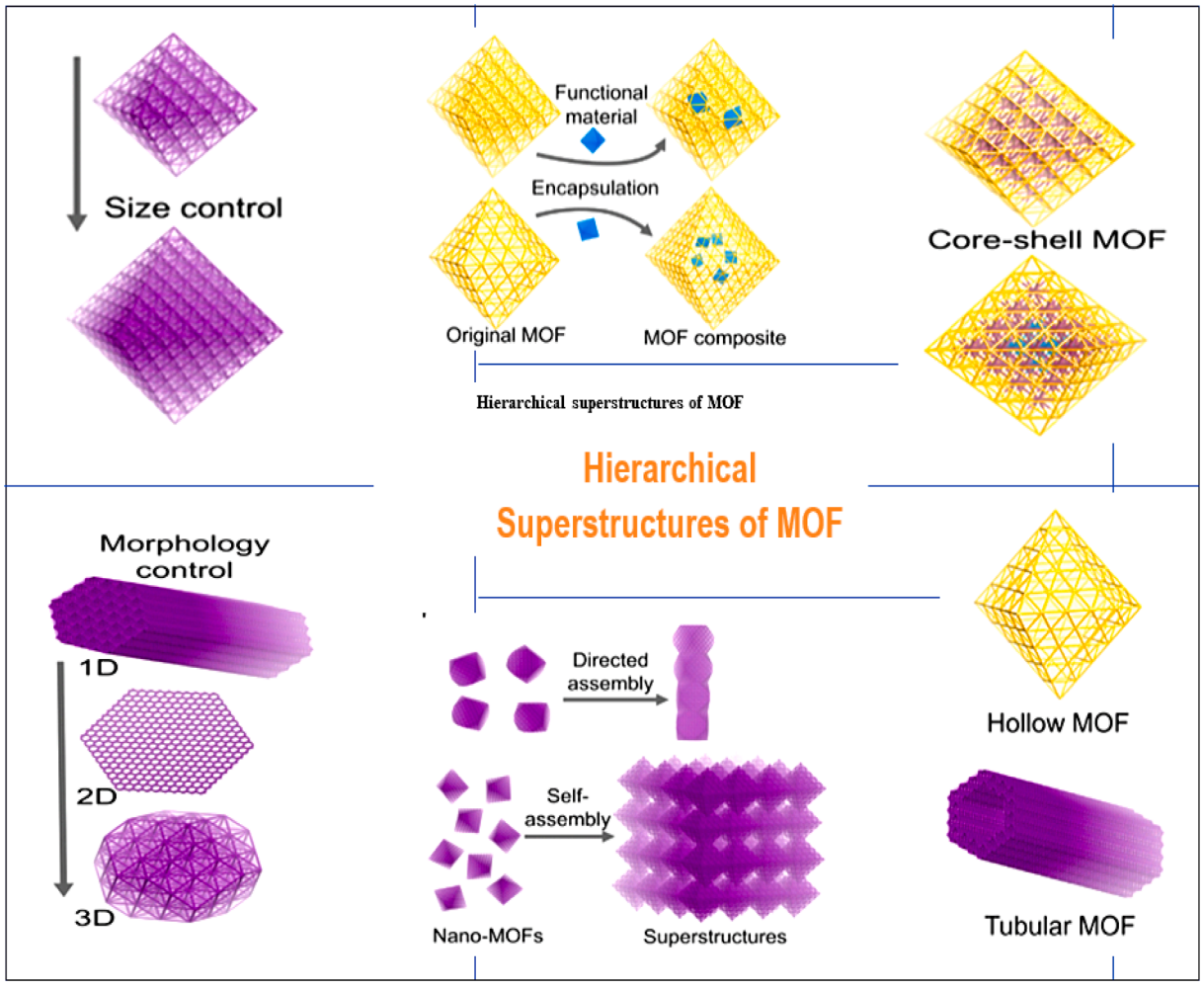

Fig. 3. Hierarchical superstructures of MOF. Adapted with permission [8] Copyright (2019), Matter.

porous MOFs, offers various benefits in increasing diffusion rates, providing active sites for the reactions, modifying the reaction directions, etc. [8] It is discovered that packing density of the MOFs is gradually increased through the process of developing MOF from crystallites to superstructures. Also, the morphology of the MOF can be modified by changing the rate of growth and nucleation. Changes in the crystalline states of MOFs have resulted in unique features of controllable pore sizes adapting different chemical reactions [9].

It has been found that the functionality and properties of MOF can be controlled by changing its physical parameters such as morphological characteristics, composition, and sizes. Principally, MOFs with well-defined sizes and shapes are used as a construction basis to synthesize various forms of MOFs. For an instance, different kinds of hierarchical styles such as hollow, core–shell, hybrid composites, and porous MOF constituents are developed **(**Fig. 3**)**. In addition to morphological control as 1D, 2D, and 3D modes, the properties of MOFs including selectivity, catalytic activities, and diffusion kinetics can be improved by controlling surface characteristics, porosity, topology, and functionality. Considering the specific features of MOF, framework structure and constant porosity are two major requirements to maintain the constancy of properties of the material, which are more relevant for certain purposes. However, several measures have been used for enhancing the material characteristic features of surface area, stability, flexibility, and conductivity. In that sense, several factors influence the stability of the MOF. Building blocks (metals, clusters, ligands), coordination geometry, surface features of pores (ex: hydrophobicity), and working environmental situations (ex: temperature, pH, pressure, media) are some of them. So, it is necessary to pay attention to those factors while preparing MOFs [8,10].

Apart from these features, MOFs are often useful as precursors for the development of single-atom catalysts (SACs) because of their porous architectures and high degree of designability. In particular, SACs with catalytically active MN_x centers have been fabricated using N-rich ZIFs as suitable precursors. Nevertheless, the microporous nature of the majority of ZIFs results in derived single-atom catalysts (SACs) that possess restricted porosity. This limitation significantly hampers the transfer of mass for reactants and the ability to reach active sites. For instance, a suitable framework for the advancement of SACs with a three-dimensional ordered macroporous structure was developed. The electro/photocatalytic transformations of small molecules, such as CO_2, H_2O, and O_2, have been found to be more efficient when utilizing this three-dimensionally ordered macroporous SACs compared to their microporous counterparts. In another study, **Yao et al.** employed an ordered macroporous ZIF-8@ZIF-67 composite material to synthesize a Co/NC catalyst featuring 3D ordered macropores and hollow walls. In order to optimize the exposure of active Co sites to reaction substrates, the resulting Co/NC material has the ability to enhance long-distance mass transfer, while the presence of hollow walls can enhance the local accessibility of these active sites. The catalyst exhibited significant enhancements in both catalytic activity and selectivity for the hydrogenation of furfural to cyclopentanol [11].

Further, **Yao et al.**, successfully anchored Co single sites on a nitrogen-carbon substrate with a 3D ordered macroporous structure (Co-SA/3DOM-NC), using pyrolysis treatment of bimetallic ordered macropores-ZnCo-ZIF. The catalyst under investigation exhibits a uniform distribution of single atomic Co sites and interconnected ordered macropores. This catalyst has shown remarkable catalytic activity in the oxidative esterification reaction. The experimental findings provide evidence that the CoN_4centers exhibit significant inherent reactivity, while the 3D-ordered macroporous architecture facilitates efficient diffusion of reactants and enhances the availability of uniformly dispersed Co atoms. Consequently, this synergistic impact contributes to the exceptional catalytic efficacy observed in the Co-SA/3DOM-NC material [12,11].

On the other hand, MOFs are considered to be very suitable for comprehending the relationship between structure and performance. This is primarily attributed to their precisely defined crystal structures, which facilitate the accurate characterization of atomic arrangements and enable computational modelling. The catalytic utility of MOFs is hindered by the presence of organic linkers inside their crystalline frameworks, which obstruct the inorganic nodes and prevent the availability of open sites for substrate chemisorption. The elimination of labile ligands by means of heating or evacuation enables the inorganic nodes containing coordinated labile ligands, such as solvent molecules and modulators, to generate coordination unsaturated sites. These sites serve as Lewis acid catalysts inside specific MOFs. Nevertheless, the presence of organic linkers might occasionally obstruct the coordination spheres of the inorganic nodes, leading to reduced activities of MOFs [13,14]. The removal of organic linkers can lead to the exposure of inorganic nodes, albeit with the potential consequence of framework collapse and a notable decrease in porosity. In this context, **Chen et al.** [15] successfully synthesized "quasi-MOFs," which possess a unique structure that is within the intermediate realm between MOFs and metal compounds, including metal oxides, nitrides, sulphides, and phosphides. The obtained outcome demonstrates that quasi-MOFs possess the ability to not only expose inorganic nodes but also retain a portion of the framework's porosity. The inorganic nodes that are exposed have the ability to act as active centers for catalysis independently, or they can work as catalysts in collaboration with other species, such as metal nanoparticles (NPs) or metal oxides. The partially intact porosity structure facilitates the transportation of substrates to the reaction centers and the subsequent desorption of the resultant products. The connection between the inorganic nodes and organic linkers in MOFs can be partially disrupted through several post-treatment methods, including heat transformation, acid/base treatment, solvent-assisted ligand exchange, and mechanical manipulation. In particular, the thermal transformation of MOFs is a robust methodology for the synthesis of diverse functional materials. The thermal transformation of MOFs has been demonstrated for the production of carbon materials in 2008, metal oxides in 2010, and quasi-MOFs in 2018. The achievement was attained through meticulous control of pyrolysis variables, such as temperature and gas composition. There is an increasing inclination towards improving the catalytic efficacy of mono- and bimetallic MOFs and their composites by deliberately converting MOFs into quasi-MOFs. The quasi-MOF-immobilized metal nanoparticles (NPs) have been widely utilized in synergistic catalysis [16].

With the widening variety of applications, several strategies have been found that can be used to tune the properties of MOFs, including stability, conductivity, and porosity. Some researchers have reported that the chemical and physical properties of MOF can be adjusted by using post-synthetic modification methods such as removal, transfer, and exchange of linkers/metals from the framework. The surface chemistry of the MOF can be altered with the changes in the size of the crystallite and the crystalline phase. In addition, the superior chemical and thermal stability of MOFs can be achieved by using redox-inactive metals with short-length and high-stiffness linkers. Also, adding flexible ligands, controlling crystal sizes, building multi-metallic frameworks, and improving the strength of metal–ligand interactions contribute to enhancing the mechanical properties of MOFs. Although at the origin, MOFs are highly porous with a large surface area, the pore size and topology of the framework can be subtly modified by choosing the proper nodes and ligands [17].

Considering the wide range of applications, it is necessary to keep the structural properties of MOFs constant while using different media including neutral, acidic, and basic conditions. The type of building units, nature of the pores, working conditions, and coordination geometry are several factors thataffect maintaining stability. It is well-known fact that MOFs should be water-stable while used in industrial uses. So, more research has paid the way to find water-stable MOFs. According to the hard-soft acid-base (HSAB) theory, highly stabilized MOFs can be synthesized using high-valent metal ions (hard Lewis's acids) including Cr^{3+}, Fe^{3+}, Zr^{4+} and carboxylate-based linkers (hard Lewis bases) to

overcome this issue [10].

Because of its wide range of possible applications, MOFs' chemical, thermal, and mechanical stability are of paramount relevance. If a MOF can tolerate the effects of a wide variety of environmental factors, including water, solvents, acids, bases, and aqueous solutions containing coordinating anions, then it is chemically stable. MOFs are both thermally and mechanically stable, meaning that they do not undergo significant structural changes when subjected to heat, vacuum, or pressure. However, most of the reported MOFs are not very stable under those circumstances. This defect reduces the MOFs' practical value. The significance and urgency of this issue has led to a great deal of effort being put into the research, development, and implementation of stable MOFs. Thermodynamic, kinetic, and other operating environment characteristics all contribute to MOFs stability under normal conditions [18,19]. The thermodynamic characteristics depend critically on the strength of the coordination link between the metal and ligand.

The stability of coordination bonds can be predicted using Pearson's HSAB theory. In the de novo synthesis of MOFs, ligands with a high *p*Ka (like azoles) are ideal for synthesizing strong frameworks with low-valent metal ions, while linkers with a low *p*Ka (like carboxylic acids) tend to connect with high-valent metal ions to produce tabular structures. The metal clusters in many MOFs, notably MIL-101(Cr), provide them with excellent chemical stability [20]. However, while the metal cluster and framework architecture remain unchanged, the chemical stability of various MOFs decreases with the lengthening of the linker and the widening of the pore size (as discovered in UiO-66series, SUMOF-7series, etc.) [21]. This is because of kinetic parameters such the rigidity of the linker, the number of coordination, the hydrophobicity of the surface, the level of penetrability of the framework, etc. Dense, rigid frameworks comprised of rigid, densely coupled building components (metal ions/clusters and ligands) are often the most stable structures possible. Because surface hydrophobicity prevents water adsorption into holes and/or water condensation around the metal clusters, MOFs are more stable in the presence of water. However, the increased stability from framework interpenetration is likely due to larger steric hindrances to ligand displacement. The decreased systematic energy of the connected structure also has an effect that can't be ignored [22]. The operating environment influences MOF stability in addition to these internal considerations. The moisture-sensitive MOF-5 maintains crystallinity even after being heated at 300 °C in air for 24 h [6].Because of this, finding the best MOFs for a given application requires adjusting the criteria by which their stability is assessed.

2.2. Structure and physico-chemical properties of MOF-based composites

In the latest centuries, MOFs have attracted considerable attention due to their tunability of properties, constant porosity, facile synthetic methods, etc. The use of these materials is limited due to their low fabrication operability, stability, and weak physical strength. Typically, most MOFs are unstable in aqueous conditions leading to irreversible degradation within a few minutes when exposed to moist environments. In some cases, for storage and catalysis purposes, the use of MOFs is restricted due to the structural weakness of the poor product. As a solution that can overcome those issues, MOF-based composites are introduced. From the beginning, the study of solid state and coordination chemistry of MOFs leads to preparing and modifying MOFs into a composite with the introduction of functional components like metal nanoparticles, nanowires, nanofibers, quantum dots, polymers, polyoxometalates (POMs), carbon-based dyes, enzymes, silica and tiny biomolecules (Fig. 1) [5].It is noteworthy that generally composite materials consist of functional species (FSs) and matrix, which is considered as the leading component of the mixture [23]Some studies have been conducted to synthesize MOF composites with matrix materials or FSs to not only improve the properties of MOFs but also to expand their use in a wide range of fields such as energy storage, sensors, environmental, medical applications, etc. Thus, it has been found that the functions, stability, and durability of MOFs can be enhanced through changes in structural architecture. However, research related to the characterization of MOF composites is relatively less compared with that of pure MOF materials [24].

There are two ways to fabricate MOF composites. By integrating MOFs with other appropriate compounds, large complex structures can be made while thin films of composites can be obtained by dropping the MOFs onto two-dimensional curved/ flat surfaces. Considering the structure of the MOF composite made with FSs, the MOF is inserted into the flexible matrix in a crystalline sequence. The structure of this composite contributes to improving the adaptability of MOF components as well as their recovery and reuse. This leads to the development of their applications in the fields of catalysis, separation, and purification. In fact, the MOF is prepared with the matrix to support the FSs that are accommodated in the composite. Although the arrangement of the MOF limits the assemblage and transfer of the components within the MOFs framework, it helps to modify the reaction routes leading to novel properties [23].

As a revolution in MOF composites, some researchers discovered that combining MOF with polymers can create composites with greater benefits than using pure polymers or MOFs. This is because, polymers are rich with the properties of chemical, thermal, and mechanical stabilities. In polymers/MOF composite, polymers provide the medium for integrating MOFs into engineered structures [25].In addition to polymers, some inorganic resources such as porous alumina and porous silica are used as FSs. The synthesis of MOF composite using polymers is very convenient compared to others. This leads to attracting high demand for industrial-scale productions. Polymers can be integrated into MOFs in different modes as films, binders, or mixed-matrix membranes. The structure of the composite has been developed to improve the performance of their applications and to adapt to exposure to extreme conditions such as toxic chemicals, fire, and infectious **(**Fig. 4**a)** [25,26].

Based on the synthesis of MOF/polymers composite, they can be classified into two types as MOFs as matrix and MOFs as FSs. So, the methodology is an important factor that determines the surface area and crystallinity properties of MOF-based composites. Solution blending (SB), electrospinning, surface coating, and in-situ growth are some of the methods which are used to produce MOF composites **(**Fig. 4**b)**. In polymers-based MOF composite can be easily made using SB methods because of the higher solubility of polymers in solvents. However, there is a high probability to occur uncontrollable defects having holes while fabricating MOF/polymers composites via the SB method. As a solution, N-methyl-N-(trimethylsilyl)-trifluoroacetamide has been used as the silylating agent to increase the affinity between MOF and polymers [23] The fiber form of MOF composites can be made via the electrospinning technique. Herein, through changing the concentration of polymers and the ratio of MOF: polymers, the loading amount of MOF and the diameter of the fiber can be controlled. The most advantages of this type of composite, compared to integrated-matrix films are, providing easy access to the active sites of MOFs and enhancing the rate of molecular transfer across the materials. By using different techniques, MOFs are grown in three ways: (i) inside, (ii) attached, and (iii) on the fibers. In that sense, the MOF-first strategy structure can be expanded into several morphologies as embedded, diverged, attached, bulged, and agglomerated through tuning the interaction between MOF and polymer in the composite **(**Fig. 4**c)** [25].

Apart from polymers, several studies have found that several types of metal, mostly d-block elements like Ag, Au, Ni, Ga, Pt, Ru, and Pd have high capability to form MOF composites. This is because of their reactivity with acid-base compounds, and their ability to form complex structures. It has been found that more than one metal can be used in composites of MOF. In this regard, coprecipitation, solid grinding, gas phase infiltration, impregnation, and direct encapsulation are some of the techniques which are applied for the synthesis of metal/MOF composite. Moreover, some graphene-based materials, such as graphene oxide, which acts as a template, are also widely used to build

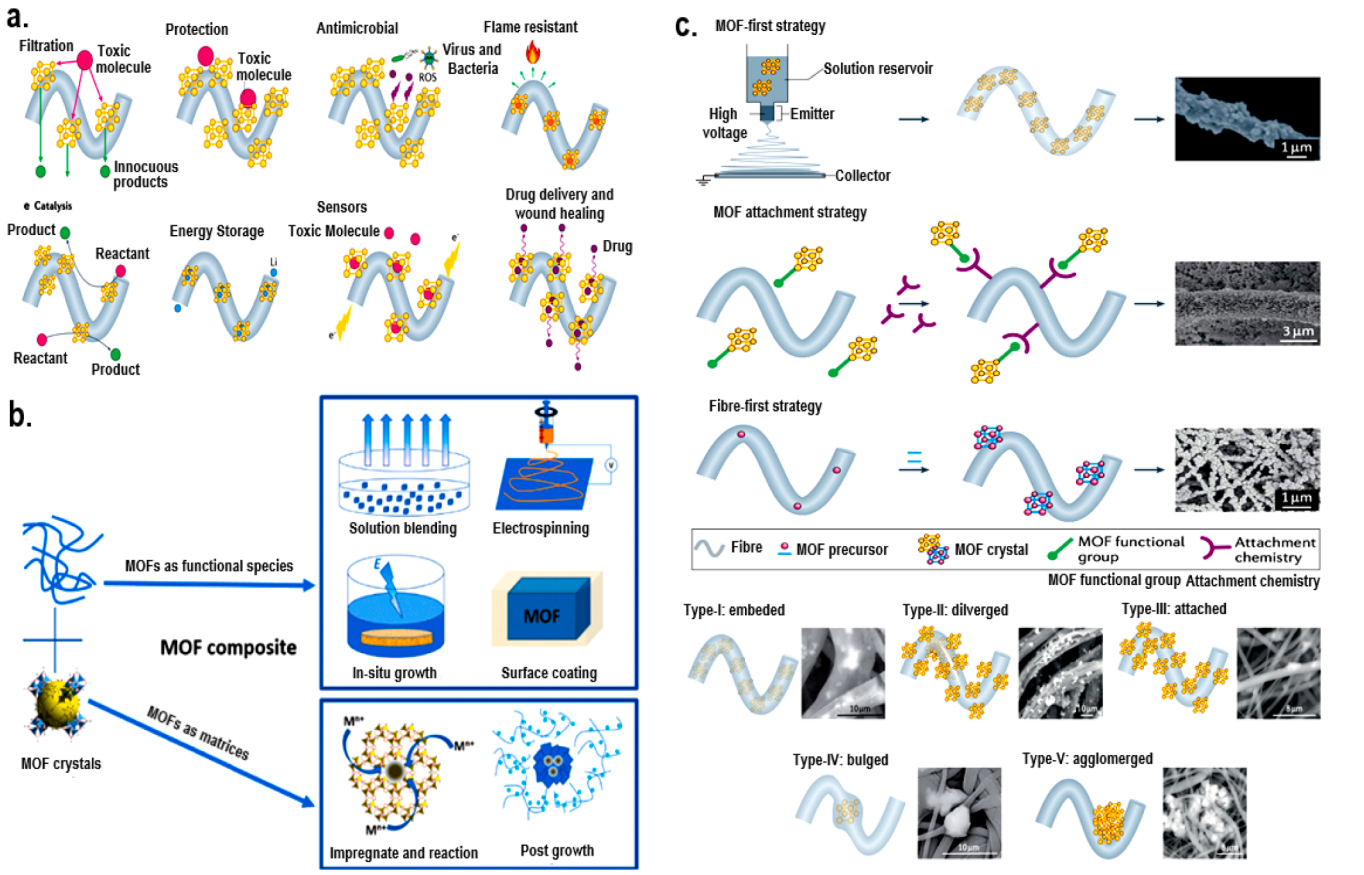

Fig. 4. (a) Structural changes of fibrous MOF/polymers composite based on the application, adapted with permission [25], Copyright (2021), Nature (b) Types of MOF/ matrix composites based on synthesis technique, adapted with permission [23] Copyright (2015), Nanoscale, (c) Morphologies of MOF-fiber composite, Adapted with permission [25],Copyright (2021), Nature.

composites. [19]. Overall, the morphology, size, and yield of the composite can be controlled by tuning the properties of MOF and composing materials.

3. Applications of MOF-based composites

Based on the previously published reports, it can be concluded that MOFs have gained attraction as one of the fastest-developing porous materials due to their ability to tune morphology, types of inorganic linkers, and organometallic species. By combining MOFs with various suitable materials, properties such as stability, morphology, production kinetics, and physiochemical features can be improved as discussed in (Section 2). Therefore, the demand for these MOF composites has expanded in a wide range of applications including catalysis, adsorption of organic/ gas molecules, electrode materials for energy storage, drug delivery, luminescence, separation, CO_2 photoconversion, and nanomaterial carriers, etc [27].

In chemical reaction systems, heterogeneous catalysts have extensive attention due to their ability to be easily separated from liquid-phase reactions. Nevertheless, the accumulation of particles in the synthesis of this type of catalyst leads to the disruption of the catalytic actions and reduction of the surface area. In this respect, many studies have focused on finding ways to improve the catalytic performance of heterogeneous catalyst materials. Thus, this research topic is updating day by day with the novel innovation around this. Formulation of composites with functional materials helps to enhance active sites and morphological characteristics. Accordingly, MOF can be considered an effective material for this application. There are several reasons why MOFs are unique in showing excellent functions as support material in composites. The first reason is the structural features of high porosity, uniform pore structure, and high surface area of MOF. Second, the uniform pore structure of MOFs acts as a shield enabling selective catalysis. A third reason, the presence of unique functional groups in the organic chain of the MOF affects the restriction of the movements of the catalytic active elements, extends the life span of the catalysts, and prevents the loss of high-priced metals. MOFs possess superior photocatalytic activities due to their strong light absorption, resulting in high utilization efficiency of solar energy. In addition, the possibility to form different structures of MOFs by changing metals and ligands or by composing with different active materials facilitates the acceleration of catalytic activity of composite [28,29]. The most significant features of MOF-based composite as a heterogeneous catalyst are stability, reusability, and high activity [30].Among the guest components, the incorporation of POM into MOFs has increased demand as catalysts for many research directions. Apart from the unique characteristics of MOFs, the strong correlation between MOF and POM (ex: hydrogen bond, electrostatic interactions) leads to avoiding the dissolution of POMs [31]. This leads to the use of this composite in many of applications. This section highlights various catalytic applications of MOF-based composites. These applications encompass thermocatalysis, specifically oxidative fuel desulfurization and oxidation of organic compounds. Additionally, photocatalysis is discussed, with a specific focus on photocatalytic reduction of CO_2. Electrocatalysis is also explored, particularly in relation to the hydrogen evolution reaction (HER), oxygen evolution reaction (OER), and CO_2 reduction reaction (CO_2RR). Lastly, the section delves into electrochemical energy storage, specifically in the context of lithium-ion batteries and supercapacitors. Furthermore, we also placed significant emphasis on the use of MOF-based materials in the field of environmental remediation [32].

3.1. Thermocatalysis

Catalysts for a wide range of organic reactions, including selective oxidation of hydrocarbons, cycloaddition of CO_2, hydrogenation of unsaturated hydrocarbons, epoxidation of olefins, and one-pot cascade reactions can be proceeded with pure MOFs and MOF-based materials with tunable metal nodes and organic ligands [33,34]. However, the poor catalytic activity is due to the substrate molecules being unable to freely diffuse through the pristine MOF crystals and contact the core active sites. In contrast, MOF-based composites are promising thermocatalytic models due to their higher surface area, more accessibility to exposed active sites, and open metal surfaces than certain standard pristine MOF crystals. In this section, we particularly focused on the recent advances on the catalytic uses of MOFs-based materials for oxidative fuel desulfurization, and hydroxylation and oxidation of organic compounds [32].

3.1.1. Oxidative fuel desulfurization.

Over the last few decades, the emission of toxic sulfur oxide (SOx) gases from fossil fuel combustion has caused several environmental concerns such as acid rain, air pollution, catalyst deactivation, and equipment corrosion. In liquid fuels, sulfur (S) can exist in several forms like sulfides, disulfides, mercaptans, thiophene, benzothiophene (BT), dibenzothiophene (DBT), 4,6-dimethyl dibenzothiophene (4,6-DMBT), benzonaphthothiophene, etc. [35].Thus, the removal of sulfur from petroleum products is indeed a challenging task. So, it is necessary to find a way to produce clean fuels with low sulfur content (<1ppm) required for fuel cell applications. In that sense, hydrodesulfurization [36], extraction desulfurization [37], bio sulfurization [38], adsorption desulfurization [39,40],supercritical water desulfurization [41], evaporative desulfurization [42], and oxidative desulfurization (ODS) [43], are discovered as top seven techniques which used to desulfurize the fossil fuels. Among those, ODS is in high demand in the removal of sulfur (S)-containing aromatic compounds below 10 ppm because of their relatively low cost, high efficiency, mild working conditions, and no use of hydrogen. This process takes place in two main steps: (i) oxidization of organic species to sulfones/ sulfoxides, (ii) removal of oxidized products by adsorption/ extraction into the polar solvent [44]. During oxidization, divalent S atoms are converted to hexavalent S (sulfones) through the electrophilic addition reaction. Typically, H_2O_2 is used as oxidizing agent due to its low price, environment friendliness, and high availableness. The products obtained after oxidation are more polar than sulfides. This is because, some of the polar solvents including acetonitrile, methanol, N- methyl pyrrolidone (NMP), isopropanol (IPA), and dimethylformamide (DMF) are used in the extraction process. Among those, the separation using NMP and DMP is very expensive and difficult, and acetonitrile is considered as the best solvent in the separation of sulfones by distillation and additional extraction [45]. Metal oxide, MOF, metal complexes, covalent organic frameworks, ionic liquids, and biocatalysts are some of the catalysts used for the ODS process. In that sense, the role and recent progress of MOFs and their composites in ODS are briefly reviewed in this section.

Due to the characteristic features, different varieties of MOFs like pristine, bimetallic, and composite materials are used as catalysts/ supports in the ODS process. Typically, most MOFs that are used in the ODS method are made with transitional metals such as Ti, V, Zr, Co, Cr, and Fe. Herein, NU-1000, UiO-66, UiO-66(Zr)–NO_2, HP-UiO-66, MIL-125, MIL-101, MIL-47, NH_2-MIL-125, TMU-10, TMU-12, and NH_2-TMU-53 are some of the examples for MOFs which show catalytic activity during ODS process. Depending on the pore size, crystal phase, and atomic coordination, the performance of each of the above MOF types varies. This can be improved by forming open metal sites and defect sites on the structures [35]. However, through the synthesis of heterogeneous catalysts by composing MOFs with various compounds which have catalytic reactivity in oxidative reactions gives better performance in the ODS technique. Many studies have found that various types of POMs have a high potential to be incorporated with MOFs to play the role of a heterogeneous catalyst. This is because MOFs have highly porous structures which provide space for catalytic active POMs. Typically, most studies have been carried out to eliminate the most refractory sulfur-containing compounds from fuel, like DBT, BT, and 4,6-DMBT using the ODS process. The reactivity of these three molecules is increased from BT < 4,6-DMBT < DBT. The reactivity is low due to the lower electron density of BT, while the other two have relatively higher densities compared to BT. Here, the steric hindrance caused by the methyl groups of 4,6-DMBT interferes with the interaction between the sulfur molecules and the oxidant/catalyst. Although DBT is less dense compared to 4,6-DMBT, it shows higher oxidation reactivity due to the presence of alkyl groups on it. In most cases, acetonitrile (MeCN) is used as an extractant due to its high extractability, faster desulfurization rate, and better catalytic efficiency [46].

For an instance, Ribeiro *et.al* synthesized a composite by combining tetrabutylammonium (TBA) salt of Tb $(PW_{11})_2$ with MIL-101(Cr) to catalyze the ODS process. In that study, three different polar solventswere used to extract non-oxidized sulfur into the organic phase. This research group has discovered that removal of DBT into extractants varied as IPA (54 %) < MeCN (63 %) < DMF (84 %) in the presence of Tb $(PW_{11})_2$ with increasing polarity of the solvents [47]. It is a quite challenge to enhance the catalytic activity in ODS at a lower value of O/S ratio. Thus, Xu-Shen Wang et.al achieved 100 % of DBT conversion at the O/S ratio (4:1) using a composite made from phosphotungstic acid (PTA) captured in the *meso*-cages of amine-functionalized MOFs [MIL-101(Cr)]. Further, they have found that the rate of oxidation can be improved by increasing the reaction temperature. In the presence of PTA@MIL-101(Cr)–NH_2, the elimination of DBT changes with the polarity of solvent as 57 % and 87 % by MeCN and DMF, respectively [48]. In addition to this group, Lin et.al also found a way to remove DBT completely within 30 min at the O/S ratio (5:1) using 42 %PTA@MOF-808A composite. These studies have proven that the synergy of metal clusters, host MOF and guest PTA can promote the catalytic activity of the system leading to ultradeep desulfurization. This composite showed high stability indicating no decrease in catalytic performances even after five consecutive reaction cycles. Considering the high recyclability, chemical stability, and environmental sustainability, 42 %PTA@MOF-808A is a more effective heterogeneous catalyst for the ODS process compared to other POM@MOF composites [44].

Moreover, Li and co-workers discovered a POM@MOF-199@MCM-41(PMM) composite to accelerate the ODS method. By changing the mass ratio of materials in $PMo_{12-x}W_xO_{40}$ with respect to MCM-41, they found that the $PMo_6W_6O_{40}$@MOF-199@MCM-41 composite showed better catalytic performance in the ODS process. This work was slightly different from others as sulfur compounds were oxidized by O_2 resulting in 98.5 % of DBT conversion [49]. Later, a heterogenous catalyst of POM@MOF for ODS was designed by Peng et.al by using Keggin-type PTA ($H_2PW_{12}O_{40}$) and UiO-67 as host MOF. The specialty of this composite was its ability to be recycled and reused for eight successive runs without loss of catalytic activity [50]. Recently, Wei.et *al* also synthesized a Keggin type POM based rht-MOF-1 composite which can be applied to ODS. In that study, $H_{3+n}PMo_{12-n}V_nO_{40}$ was used as POM and three different composites were analyzed by varying the value of n from 1 to 3. From that, PMo_9V_3@rht-MOF-1 showed the highest catalytic reactions leading to 96 % of sulfur removal [51], When comparing all the results of experiments on different types of POM-based MOF composites, it can be concluded that these composites exhibited excellent catalytic performance for ODS, providing high chemical stability with recyclability and regeneration characteristics (Table 1).

3.1.1.1. Hydroxylation and oxidation of organic compounds. As novel applications of heterogeneous catalysts, MOF-based composites have been involved in various chemical reaction phenomena in organic chemistry including hydroxylation, oxidation, hydrogenation, and

Table 1
Comparison of the optimal reaction conditions of different POM@MOF catalysts.

Catalyst	Feedback	Oxidant	Extractant	Reaction Temperature (^{0}C)	Reaction Time (min)	O/S molar ratio	S removal %	Ref.
Tb (PW_{11})$_2$@MIL-101(Cr)	DBT, 1-BT, 4,6-DMBT in *n*-octane (500 ppm- S)	H_2O_2	DMF/MeCN/ IPA	50	120	50	100	[37]
PTA@MIL-101(Cr)–NH_2	DBT, BT, 4,6-DMDBT in *n*-heptane (950 ppm- S)	H_2O_2	DMF/ MeCN	50	240	4	100	[38]
PMo6W6O40@MOF-199@MCM-41	DBT in octane (2000 ppm- S)	O_2	–	85	180	–	98.5	[40]
PW_{12}@UiO-67	DBT, BT, 4,6-DMDBT in *n*-heptane (1000 ppm- S)	H_2O_2	MeCN	70	60	13	99.5	[41]
42 %PTA@MOF-808A	DBT in an*n*-octane (1000 ppm- S)	H_2O_2	MeCN	60	30	5	100	[39]
Keggin-POM(PMo_{11}V1) @rht-MOF-1	DBT, BT, 4,6-DMBT in *n*-octane (1000 ppm- S)	H_2O_2	MeCN	70	50	12	90	[42]
PMo_{10}V2@rht-MOF-1	DBT, BT, 4,6-DMBT in *n*-octane (1000 ppm- S)	H_2O_2	MeCN	70	50	12	92	[42]
PMo_9V3@rht-MOF-1	DBT, BT, 4,6-DMBT in *n*-octane (1000 ppm- S)	H_2O_2	MeCN	70	50	12	96	[42]

epoxidation of organic compounds. These processes can be promoted by developing the reaction of MOF-based composites with oxygen/oxo/ hydroxyl groups containing compounds. The performance of those modified catalysts is enhanced with the changes in the surface and morphological characteristics of the composites. To date, many research works have been carried out on the development of MOF-based composites for each application. Thus, this review is restricted to only a few recent specific examples which are briefly discussed in the following section.

As an oxidation reaction, hydroxylation (HL) of organic compounds can be considered an eco-friendly method resulting dihydroxybenzenes (DHB) as a major product reacting with H_2O_2. Basically, MOF-based composites act as catalysts to accelerate these reactions. There are several studies for heterogenous catalysts in hydroxylation using different types of metal complexes in the MOF cage to oxidize the phenol, styrene, and cyclohexene, using H_2O_2 as an oxidant. In this type of application, the catalytic activity occurs with the hydroxylation of compounds and decomposition of H_2O_2 molecules. It has been discovered that most of the catalysts exhibit high selectivity in the production of phenol [30]. Sun *et al.* discovered a radical capture mechanism for the hydroxylation of the C–H bond in benzene into phenol using MOF-derived Cu_graphene heterogeneous catalyst in the presence of H_2O_2 [52].During this route, the Cu_2O-rGO catalyst plays a vital role in both $^{\bullet}$OH generation and $^{\bullet}$C capture(Fig. 5**a**).Hydrogen atom transfer (HAT) method initiated by oxygen-centered radical ($^{\bullet}$OH) to form carbon-centered radical ($^{\bullet}$C) is mainly involved in this catalytic oxidation phenomenon. In this work, they discovered a unique mechanism for C–H bond hydroxylation involving the conversion of $^{\bullet}$OH to $^{\bullet}$C with the contribution of a Cu-based catalyst **(**Fig. 5**b)**. Herein, the Cu_2O-rGO catalyst was synthesized via MOF-derived procedure using2-amino terephthalic acid. This Cu-MOF structure [Cu(BDC-NH_2)] which was fabricated by the facile liquid phase deposition method acts as a precursor in this synthesis process **(**Fig. 5**c)**. Through the hybridization of metal, particles can control the charge distribution while improving the electrical transduction of this catalyst. Furthermore, the catalytic activity of this material for H_2O_2 activation is promoted by the interaction between Cu_2O and graphene particles. In this regard, the degree of phenol formation depends only on the concentration of both H_2O_2 and catalysts. When compared with the other catalyst activities, Cu (BDC-NH_2) showed better performance in benzene HL resulting in high benzene conversion and phenol yield of 24 % and 21.2 % in percentage, respectively **(**Fig. 5**d)**. In addition, this catalyst can be reused even after 5 cycles without loss of catalytic activity and selectivity **(**Fig. 5**e)**.

In the same year, but later, Xiang *et.al* discovered MOF-5-derived porous carbon (MDPC) for phenol HL(P-HL) [52]. For the analysis of the performance, two samples of MDPC-600 and MDPC-1000 were synthesized through the pyrolysis technique under a nitrogen atmosphere, at 600 °C in an acidic medium and 1000 °C, respectively. During the carbonization process, zinc oxide (ZnO) in MOF-5 was removed to form the porous amorphous compounds providing more active sites with higher surface areas (ex: MDPC-600: 1029.5 m^2/g and MDPC-1000: 1570.9 m^2/g). Further, they synthesized a composite catalyst of Fe (III)/ MDPC by loading Fe ions into MOF-5 to determine the catalytic performance of P-HL oxidized by hydrogen peroxide (H_2O_2). In this process also, DHB and hydroquinone (HQ) are obtained as products via the hydroxyl free radical mechanism **(**Fig. 5**f)**. Based on the data of this experiment, they have concluded that Fe (III)/ MDPC-1000 showed higher catalytic activities, resulting in the greatest phenol conversion (64 %), highest DHB yield (54.3 %), and selectivity of DHB (88.4 %). In that case, this P-HL reaction of Fe (III)/ MDPC composite is occurred as three main steps: (1) Oxidation of H_2O_2 into •OH with the reduction of Fe^{+3}/Fe^{+2}, (2) Formation of·H_2O and Fe^{+3} by reacting Fe^{+2} with another H_2O_2, (3) formation of DHB and HQ by reacting •OH radicals with the carbon at the ortho and para position of phenol (**Equation 1**–**3**, Fig. 5**g**). Although Fe (III)/ MDPC composite reacts with another oxidant (*tert*-Butyl hydroperoxide/ O_2), it has been reported that only H_2O_2 supports success with this P-HL process using this composite [52,53].

Among the heterogeneous catalytic applications, the oxidation of various compounds like alcohols, and hydrocarbons become a great innovative research topic in organic chemistry. Oxidation of alcohols to carbonyl compounds has been a rather challenging reaction because it can be used as precursors in the production of fine chemicals [56]. When this reaction is catalyzed using a MOF-based compound, a carboxylic acid is formed as a byproduct. Due to the coordination structure of this compound, it can smoothly inactivate the active sites of this complex. This is the important function of the MOF composites as catalysts in this reaction. For an instance, a Pd nanoparticle-loaded composite material, Pd@Cu(II)-MOF was synthesized by Chen et al. via the solution impregnation method for aerobic oxidation of benzylic alcohol [55]. It has been reported that this material showed excellent activity (93 %->99 % conversion) and selectivity (aldehydes, >99 %) which was considered the highest value with comparing other heterogeneous catalysts **(**Fig. 5**h)**. In this Pd@Cu-MOF composite, face-centered cubic Pd nanoparticle act as the main catalytic active site for the oxidation of aromatic carbinols onto corresponding benzaldehyde. Before this work, they investigated the catalytic activity of the Pd/MIL-101 on selective aerobic oxidation of alcohols [57]. In the absence of solvent-free and alkali conditions, this oxidation reaction exhibited turnover frequency (TOF) up to 16900 h^{-1}. In that regard, open Cr sites of the MIL-101 promote the oxidation of alcohols. Later, Pd@Cu-MOF was synthesized with some modifications to improve the selectivity of the oxidation of alcohols.

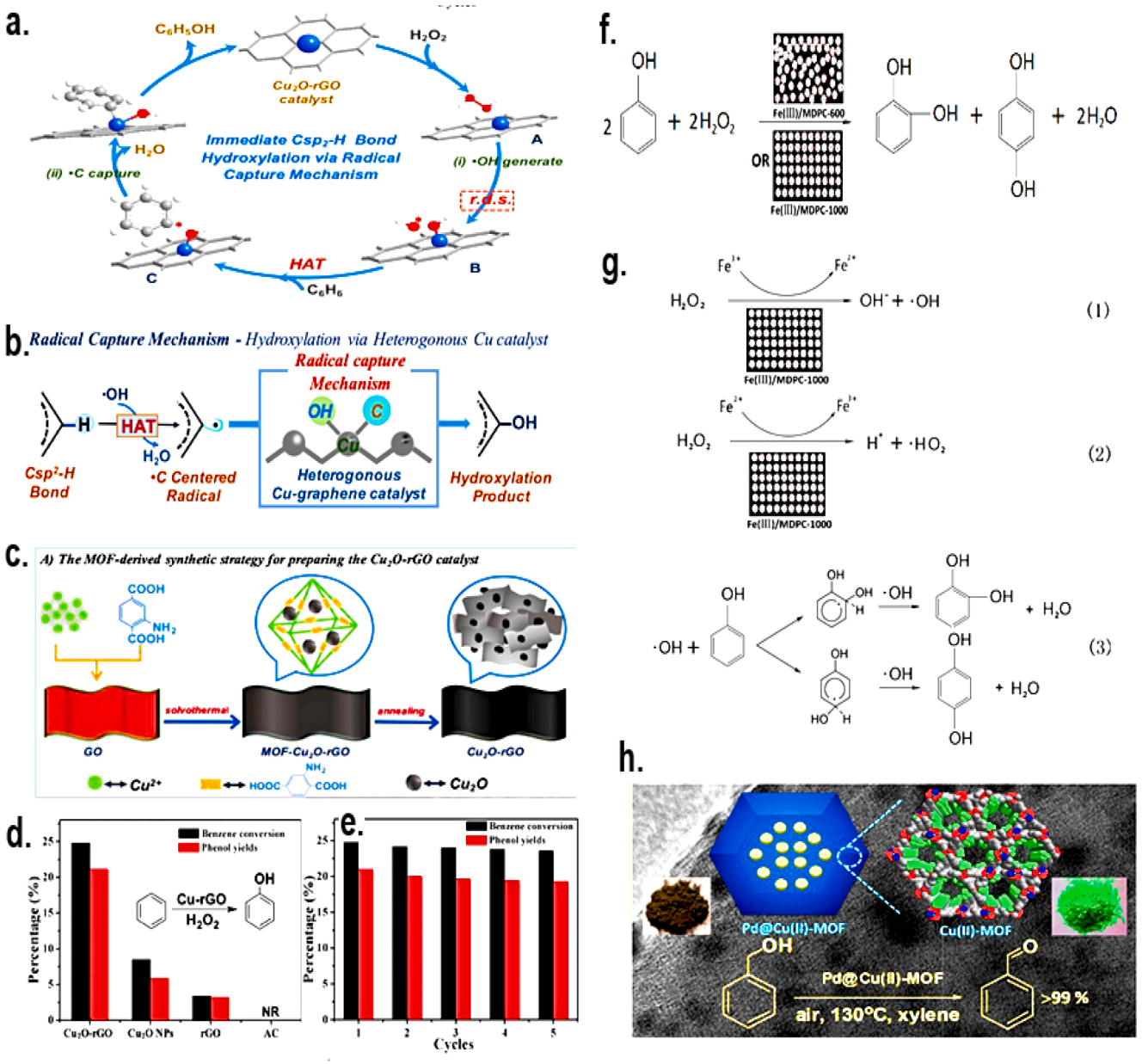

Fig. 5. Heterogenous catalytic reactions (a)Complete free radical capture mechanism for C–H bond hydroxylation using MOF derived Cu_2O-rGO catalyst, (b) Overallradical capture mechanism of benzene hydroxylation, (c) Schematic diagram of Cu_2O-rGO synthesis process,(d)Comparison of catalytic performance of Cu_2O-rGO, Cu_2O, rGO, AC in benzene hydroxylation, (e) Recycle performance of Cu_2O-rGO after 5 cycles, Adapted with permission [52], Copyright (2019), Chemical communications; (f) Overall reaction of phenol hydroxylation (P-HL), (g) Three steps of reaction mechanism P-HL of Fe (III)/MDPC-1000 with H_2O_2 oxidant, Adapted with permission [54], Copyright (2019), Chemistry Select, (h) Oxidation reaction of benzylic alcohol using Pd@Cu(II)-MOF, Adapted with permission [55], Copyright (2016), Inorganic Chemistry.

Recently, Paul and his group discovered a MOF-based composite using metal ions of Co (II) and Zn (II) to catalyze the oxidation of benzyl alcohol [58]. Co-MOF processed this reaction using a solvent-free microwave procedure whereas *tert*-butyl hydroperoxide (TBHP) acted as an oxidant. This composite showed 87 % of selectivity, 89 % yield of benzaldehyde, and 148 h^{-1} TOF. Relative to Co-MOF, Zn-based composite exhibited weak catalytic activity resulting in a value of yield, selectivity, and TOF, of 27 %, 90 %, and 45 h^{-1} respectively. In the same reaction conditions, $CoCl_2{\cdot}6H_2O$ and Zn $(NO_3)_2{\cdot}6H_2O$ showed 13 % and 5 % yield, 22 h^{-1} and 8 h^{-1}, and 64 % and 58 % of selectivity, respectively. Based on the summarized data, it can be concluded that Co-based MOF showed higher catalytic performance compared to another heterogeneous catalyst for alcohol oxidation.

In addition to alcohol oxidation, researchers have focused their attention on the aerobic oxidation of hydrocarbons catalyzed by MOF-composites. Several research works have been reported in this regard using MOF-based catalysts combined with different active materials of POMs, GO, Au so on. As a recent example of this, Tong et.al introduced a POM-MOF composite, $H_{3+x}PMo_{12-x}V_xO_{40}$@MIL-100 (Fe) (x = 0, 1, 2), to oxidize the cyclohexane into 2-cyclohexane-1-one using H_2O_2 as the oxidant [59]. From this, they finalized that this oxidation reaction can be successfully catalyzed by both composites $H_4PMo_{11}VO_{40}$@MIL-100 (Fe) and $H_5PMo_{10}VO_{40}$@MIL-100(Fe). Among them, the high cyclohexene conversion, selectivity for 2-cyclohexane-1-one, and TOF were exhibited by $H_4PMo_{11}VO_{40}$@MIL-100(Fe) as 85 %, 91 %, and 715 h^{-1}, respectively. Moreover, this compound can be reused for five runs, indicating superior recyclability. Although there are several works based on these applications, it is difficult to summarize them into one review.

Therefore, only selected examples have been briefly deliberated here.

Overall, MOF-based catalysts can be utilized as efficient materials in typical thermo-catalytic applications, like oxidative fuel desulfurization, hydroxylation, and oxidation of organic compounds, under a variety of conditions. Several strategies, including tuning of the nanoscale thickness of MOFs, abundance of exposed active sites, and lack of diffusion constraints, could be used to improve the catalytic performance of their bulk pristine MOF crystal counterparts. For real-world applications, it's important to think about how MOF-based composites hold up under harsh reaction circumstances like high temperatures or the presence of oxidizing or reducing gases. Lewis acidic sites and basic sites can be inserted into the crystal structure of MOFs to serve as bifunctional catalysts for such thermo-catalytic reactions, respectively.

3.2. Photocatalysis

Usually, photocatalytic reactions occur by separating electron-hole pairs from each other, followed by moving into catalytic active sites. In that sense, separation efficiency which is carried out through photo-inspired charge carriers is a decisive factor in this process. In this regard, the ability of MOF-based photocatalysts to respond to visible light, the locations of the conduction band (CB) and valence band (VB), the segregation of photo-generated charge carriers, and the mobilities of these charges all play a role in their catalytic effectiveness. Recent advances in MOFs have made them an attractive option for photocatalysis due to their many desirable properties. These include an abundance of exposed active sites, distinctive metal node-organic ligand interactions, an ultra-thin thickness, and the ability to tailor composition and functionalities. MOF-based photocatalysts with tunable chemical compositions and functionalities have been shown to exhibit enhanced visible-light adsorption and electron emission. Furthermore, the increased surface area and number of exposed active sites can facilitate rapid surface redox reactions during photocatalysis. To further expedite the separation of photo induced charge carriers (electrons and holes), a hetero junction between nanoscale photocatalysts and MOFs may be built to increase the stability of supported nanoscale photocatalysts without considerable aggregation.

Nowadays, the process of converting CO_2 into value-added organic substances like CO, CH_4, HCOOH, CH_3OH, cyclic carbonate, and hydrocarbon fuel using solar energy has become a promising approach to overcome the issues of global warming and energy source deficiency. This is considered an effective method of neutralizing carbon molecules. During this process, a large amount of energy is required to break the strong C = O bond and to form C–H bonds at some sites. After the catalytic process, two-electron CO, and eight-electron CH_4 reduction products were produced. However, CO_2 reduction and oxidation of H_2O in the photocatalytic system is quite challenging due to the thermodynamic stability and kinetic inertia of CO_2 molecules. Some factors including sufficient light absorbance, surface catalytic reactions, rate of charge separation, and transfer directly affect for the photoreduction of CO_2. Therefore, it is required to develop an effective material with recyclability, high photochemical sensitivity, and light absorption properties that provide better performance as photocatalysts [60,61].

However, MOFs have some limitations in terms of stability and responsiveness to light sources. Through the conjugation of various catalytically active functional materials into MOFs, the problems associated with MOFs can be overcome resulting in improved properties associated with structural changes. Especially, MOFs with metals (ex: Ag, Ni, Co, Zn, etc.) can promote photocatalytic activity by suppressing photo induced hole and electron incorporation. There are several photocatalysts such as CdS, TiO_2, graphitic carbon nitride (g-C_3N_4), and Zn_2GeO_4 which can be combined with MOFs to reduce the CO_2 into some valuable chemicals. It is noteworthy that g-C_3N_4 has a sufficient band gap, which contributes to the collection of visible light and a slightly negative conduction band and valence band with thermodynamic energy. Due to these features, recentlyg-C_3N_4 has been applied in various MOF-based composite syntheses for CO_2 reduction purposes. Shi et.al constructed a heterogenous photocatalyst of UiO-66/g-C_3N_4nanosheetsby electrostatic self-assembly technique. In addition, the solvothermal method is also used for its synthesis. This composite exhibited a high CO evolution rate of 59.4 μmol/g h indicating a higher rate of CO_2 reduction [62]. Later, Liu *et.al* found ZIF-8/g-C_3N_4 nanostructures to convert CO_2 into solar fuel [63].When comparing the results, this composite showed lower performance compared to other materials. As a further study of the composites, Xu *et.al* fabricated a BIF-20@g-C_3N_4nanosheetwith a high density of exposed B-H bonds, which is more favorable for CO_2 activation and reduction in high efficiency [64]. They further compared the properties of this composite with ZIF-8/ g-C_3N_4.Like others, the electrostatic self-assembly method was used for the synthesis of BIF-20@g-C_3N_4**(**Fig. 6**a)**. When considering the mechanism of photocatalysis, it happened due to the quick transfer of photo-generated electrons from the CB band of the g-C_2N_4 to active sites in BIF-20, preventing reconnection of electron-hole pairs. The B-H bond of BIF-20 has the ability to capture oxygen atoms from CO_2 molecules. Consequently, CO_2 reduced into CO and CH_4 near the surface due to the high concentration of photoexcited electrons released from g-C_3N_4**(**Fig. 6**b)**. During this catalytic process, the amount of CO and CH_4 evolution increased sharply with time and the rate of CO and $CH_4$was shown as 15.524 μmol $g^{-1}h^{-1}$ and 53.869 μmol $g^{-1}h^{-1}$, respectively. BIF-20@g-C_3N_4 exhibited excellent catalytic performance compared to ZIF-8/g-C_3N_4 and g-C_3N_4**(**Fig. 6**(c-e))**. Through the production of NH_2-UiO-66@ g-C_3N_4, Wang and his team were expected to enhance photocatalytic activity and stability [65]. This group concluded that composites made of NH_2-UiO-66 and hollow g-C_3N_4 showed superior properties using in-situ solvothermal technique compared to other methods including physical mixing and electrostatic assembly. A common finding in all studies is that bulk material showed poor performance compared to individual compounds.

In 2020, Zhao *et.al.* successfully produced photocatalysts by composing Ni-MOF with g-C_3N_4 which can expand the optical density of visible lights while limiting the drawbacks of MOFs to some extent [66]. In this work, two samples were synthesized using Ni-MOF and pre-modified g-$C_3N_4$with OH (Ni-MOF@ g-C_3N_4-OH) and 4-amino benzoic acid (Ni-MOF@ g-C_3N_4-AA).Comparatively, Ni-MOF@ g-C_3N_4-AA has a higher surface area of 52.58 m^2g^{-1}which leads to higher charge transmission and provides more active sites for photocatalysis. Considering the CO_2 conversion rate in each compound, it varied from g-C_3N_4 < Ni-MOF@ g-C_3N_4-OH < Ni-MOF@g-C_3N_4-AA. Furthermore, they replaced the Ni^{+2} ion in the Ni-MOF@ g-C_3N_4-AA sample with Co^{+2} and Zn^{+2} ions during in situ growth process. Overall, high catalytic properties in CO_2 reduction can be observed in Ni-MOF@ g-C_3N_4-AA due to its structural features, introduced Ni active ions, and well-modulated interfaces. As an extended this research, Han *et.al* designed a composite by using MOFs, tridentate ligand 2,4,6-tris(2-(pyridin-4-yl) vinyl)-1,3,5-triazine (TPVT), and g-C_3N_4 [60]. In this study, a high yield of reduced CO_2 (56.4 μmol/g h) was obtained using TPVT-MOF@g-C_3N_4, which was 3.2 times higher than that of pure g-C_3N_4(17.5 μmol/g h), indicating a better photocatalytic performance of this composite. Considering the mechanism, C = C bonds in MOFs and triazine rings are involved in the reduction of CO_2 and metal sites and 1,3,5-benzenetricarboxylic acid of MOFs contributes to oxidizing H_2O. However, it can be concluded that TPVT-MOF@g-C_3N_4 is a successful catalyst without using any other sacrificial agent/ photosensitizer for this application.

As a most recent innovation, in 2022, Cheng et.al discovered [NH_2-MIL-125(Ti)-Ag] composite by depositing silver (Ag) nanoparticles on the Ti(IV)-MOF to promote the selectivity of CO_2 reduction and photocatalytic activity [61]. Herein, the photocatalytic performance mainly depends on the deposition amount of Ag materials, excess contents results in lower activity because of the accumulation of materials. Typically, higher CO_2 adsorption leads to reduce more CO_2 molecules. Loading Ag molecules and having a larger surface area are the main key reasons which decide the rate of CO_2 reduction. Comparatively, this

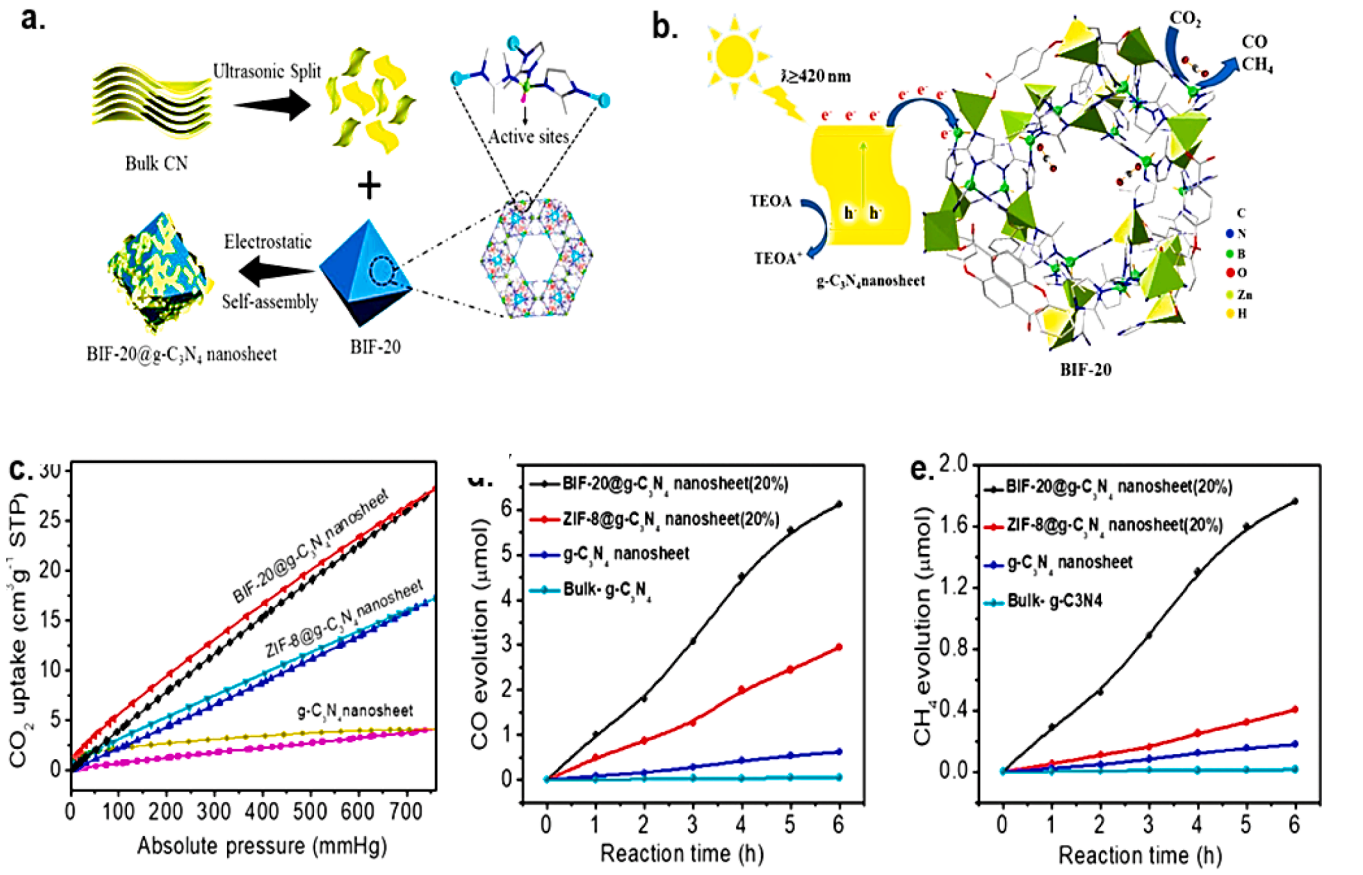

Fig. 6. (a) Method of fabrication BIF-20@g-C_3N_4 nanosheet photocatalyst, (b)Photocatalytic CO_2 reduction mechanism by BIF-20@g-C_3N_4,(c) CO_2 adsorption – desorption isotherms, (d)Rate of CO evolution, (e)Rate of CH_4 evolution, Adapted with permission [64], Copyright (2018), ACS Nano.

composite exhibited better catalytic activities in CO_2 conversion compared to its parent compound, NH_2-MIL-125(Ti). Here, all properties were compared as follows to identify the CO_2 reduction performance with varying types of heterogeneous MOF-based catalysts **(**Table 2**)**. It can be seen from the table that CO_2 adsorption increased with the combination with MOF. In conclusion, the rate of CO_2 reduction can be improved with the increase of the cage size and the nature of the pore of the catalysts.

Research on MOF-based materials as photocatalysts for CO_2 reduction has garnered significant interest, primarily due to their structural variety and physico-chemical characteristics. The findings demonstrate that photocatalysts based on MOFs have favorable photocatalytic properties and exhibit notable efficiency and selectivity in the context of CO_2RR. Nevertheless, the use of MOF-based materials in the field of photocatalysis is now in its early stages, with only a limited range of distinct MOF-based photocatalysts having been documented. In the future, the logical design of photocatalysts based on MOFs holds promise for enhancing photocatalytic performance.

3.3. Electrocatalysis

So far, there has been substantial evidence demonstrating the efficacy of MOF-based materials in various electrocatalytic processes, including oxygen and hydrogen evolution reactions (OER and HER) and CO_2 reduction reaction (CO_2RR). This section will provide a concise overview and analysis of the recent advancements in the utilization of MOF-based electrocatalysts for OER, HER, and CO_2RR.Over the last few decades, various methods have been invented to generate green energy through the conversion of the chemical energy of fossil fuels into electrical power in an environmentally friendly manner. In this regard, the demand for hydrogen as a fuel is increasing day by day due to its unique properties and its industrial uses. Hydrogen generation can be introduced as a sustainable solution for reducing the consumption of fossil fuels. Considering cost-effectiveness and facileness, water splitting can be introduced as an effective method to produce hydrogen among others including coal gasification, and photo-induced natural gas reforming [67,68]. In this process there are two types of half-reactions such as hydrogen evolution reaction (HER) and oxygen evolution reaction (OER) can be happened **(**Fig. 7**a)**. Fundamentally, the water molecule is decomposed into hydrogen and oxygen via HER and OER occurring at

Table 2
Comparison of MOF-based composite as a heterogeneous catalyst for CO_2 reduction.

Catalysts	Surface area (m^2g^{-1})	Maximum CO_2 uptake ($cm^3\ g^{-1}$)	CO evolution rate (μmol $g^{-1}h^{-1}$)	CH_4 evolution rate (μmol $g^{-1}h^{-1}$)	Ref.
g-C_3N_4nanosheet	35.14	4.11	17.5	–	[57]
UiO-66/g-C_3N_4	1315.3	32.70	59.4	–	[53]
ZIF-8/ g-C_3N_4	1177.77	17.24	24.72	3.39	[54,55]
BIF-20@ g-C_3N_4	283.67	28.24	53.87	15.52	[55]
NH_2-UiO-66@ g-C_3N_4	335	0.26	31.7	< 4	[56]
NH_2-MIL-125(Ti)	–	–	26.7	63.3	[58]

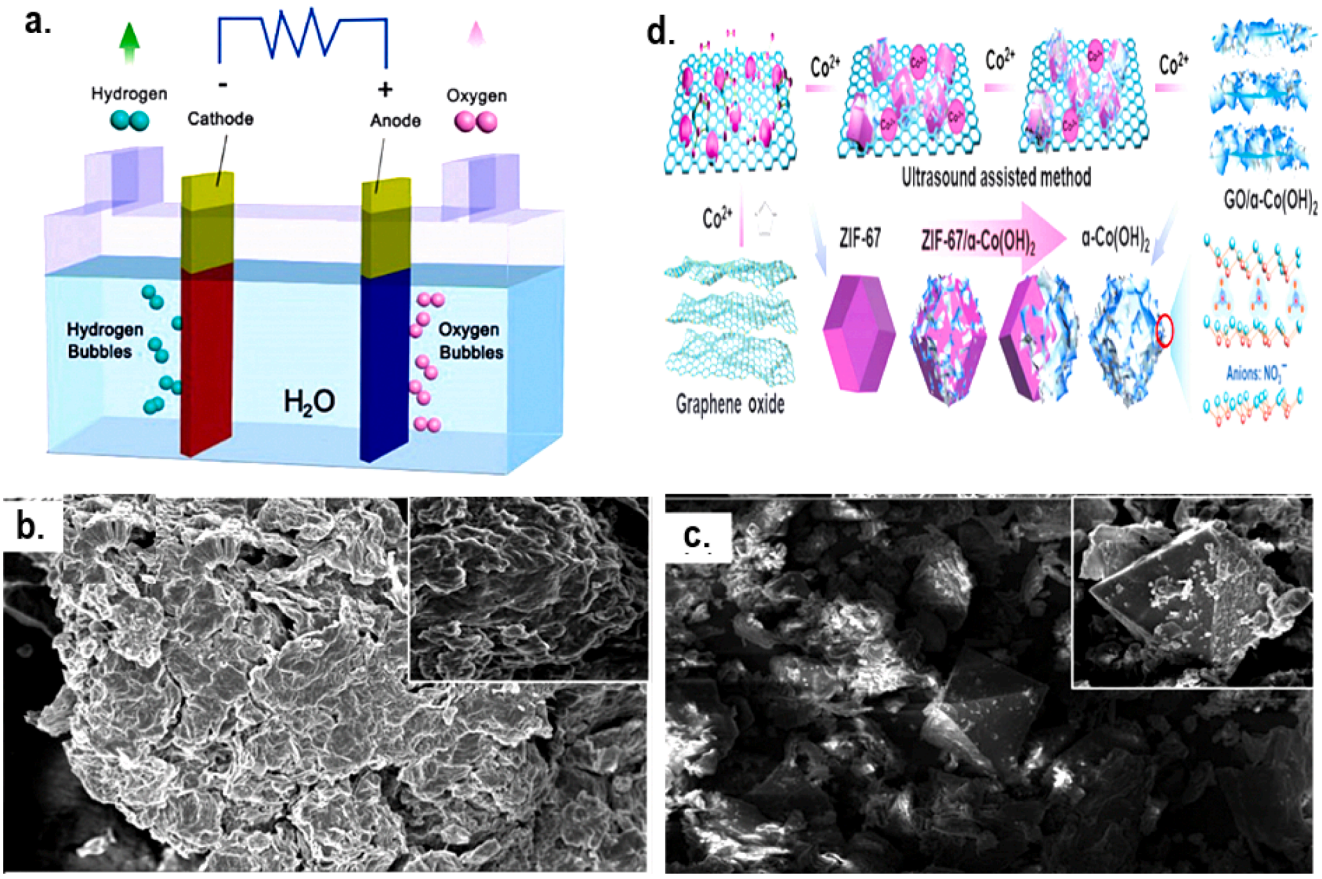

Fig. 7. (a) Demonstration of water splitting process, adapted with permission [67], Copyright (2015), Chemical Society Reviews, SEM images of (b) GO sheet, (c) MOF/GO composite, Adapted with permission [68]Copyright (2020), Int. J. Electrochem. Sci, (d) Synthesis route of ($Co(OH)_2$-GNS), Adapted with permission [69], Copyright (2020), Nano research.

the cathode and anode, respectively. Based on the reaction media, the half-reactions can be changed accordingly **(Equation 1–5)**. Theoretically, these reactions should happen within the range of 0–1.23 V at 25 °C. However, this results in an overpotential range due to the contact, and solution resistance arising from the anode, cathode, and other resistance [67].Due to this, it is necessary to find a way to conduct this process in an energy-efficient way. Different types of materials are used as an electrocatalyst to overcome the issues regarding this process.

In an acidic medium,

$$\text{Cathode}: 4H^+ + 4e^- \rightarrow 2H_2 \quad (1)$$

$$\text{Anode}: 2H_2O \rightarrow 4H^+ + O_2 + 4e^- \quad (2)$$

In neutral and alkaline solutions,

$$\text{Cathode}: 4H_2O + 4e^- \rightarrow 2H_2 + 4OH^- \quad (3)$$

$$\text{Anode}: 4OH^- \rightarrow 2H_2O + O_2 + 4e^- \quad (4)$$

Overall reaction,

$$2H_2O \rightarrow 2H_2 + O_2 \quad (5)$$

3.3.1. *Electrocatalytic H_2 evolution reaction*

The importance of hydrogen is that when it is used to generate electricity, only water is formed as a product. Herein, metal-based composite plays a vital role as an electrocatalyst in the HER process. Most HER are catalyzed using platinum (Pt-based compounds), but some drawbacks such as high-cost, and low availability limit them from further uses. In that sense, uses of transitional metal-based compounds (ex: oxides, sulfides, carbides, etc.) have been promoted as alternative materials for noble metals-based ones. Although these materials show excellent HER activity, they may be hindered by their limited active sites and low intrinsic characteristics [67]. Thus, it has been found that some enzymes which are known as hydrogenases showed better performance to improve the catalytic activity of HER. This mechanism is followed by the MOF-based composite to develop the HER activities by overcoming issues. In this regard, MOFs and their composites can be introduced as a better option due to their unique characteristics. There are three different strategies used to promote the performance of MOF as a catalyst in HER. These are, (i) applying various types of metals (ex: Pd, Ru, etc.) in MOF-derived composites, (ii) using low-cost, highly available elements (ex: Cu, Mo, Co, Fe, Ni, and so on) for preparation of composites. (iii) imitating the active sites of natural HER catalysts [67].

Recently, Makhafola *et.al* synthesized graphene oxide (GO)/ MOF composite to determine their property changes on HER [68]. Herein, Cu-based MOF (HKUST-1) was developed to examine the electrochemical behavior of HER. They observed superior catalytic activity from this composite indicating higher TOFs in H_2 production. Further, the mechanism of this process was clearly explained as three steps **(Equation 6–8)**. This reaction started with the reduction of Cu (II) to Cu(I) in the MOF/ GO composite followed by accepting a proton from the corresponding site of this complex to form a composite hydride (MOF/ GOH_{Ad}). This step is called as the Volmer reaction **(Equation (6)**. Then, H_2 gas is produced due to proton impact or interaction with other similar hydride intermediates via Heyrovsky or Tafel mechanisms, respectively **(Equation 7–8)**. The morphological changes of MOF with the integration of GO were evidently noticed by this group using SEM images. According to that, the dense flakes of graphene layers were observed in (Fig. 7**b)**. The incorporation of GO into the composite confirmed the formation of octahedral crystals of MOF/GO in (Fig. 7**c)**. This exhibited

an abrasive and rough surface of the MOF which occurs due to the chemical reaction between the Cu meal of MOF and oxygen-holding functional groups of GO [68].

$$Cu^{+2} - MOF/GO \rightarrow Cu^{+} - MOF/GOH_{ad} \quad (6)$$

$$Cu^{+} - MOF/GOH_{ad} \rightarrow Cu^{+2} - MOF/GO + H_2 \quad (7)$$

$$Cu^{+} - MOF/GOH_{ad} + Cu^{+} - MOF/GOH_{ad} \rightarrow 2Cu^{+} - MOF/GO + H_2 \quad (8)$$

3.3.2. Electrocatalytic O_2 evolution reaction

As an effective reaction in energy conversion and storage systems like metal-air batteries, water splitting, and fuel cells, OER has attained attractive interest in modern days. However, some factors including the use of expensive metal-based electrode materials and slow kinetic effect for the effectiveness of the process, lead to the limitation of industrial-scale applications. Due to these issues, finding a low-cost, high-efficiency catalyst in OER has opened a new avenue for research in this field. To date, various types of electrode materials are developed to overcome those issues. Typically, Co, Ni, Ir, and Ru-derived MOF composites are commonly used as electrocatalysts to tune the performance of OER [69,70]In electrolysis application, MOF hinders electrical conductivity due to its morphological features. Thus, pyrolysis at higher temperatures more popular technique among the various methods applied to resolve this issue. Furthermore, the combination of MOF with more surface-active material brings it to better catalytic activity with higher conductivity [69]. Recently, MOFs-derived composite based, sandwiched-like structured electrocatalyst ($Co(OH)_2$-GNS) for OER was synthesized by the Huang group using an ultrathin layered α-$Co(OH)_2$ derived from MOF decorated with GO [70]. During the synthesis process, the product of hydroxides with interlayered NO_3^- ion was formed from dodecahedral ZIF-67 tetrahedrally coordinated with the Co^{+2} compound **(**Fig. 7**d)**.

After the self-conversion process, the obtained $Co(OH)_2$-GNS exhibited greater OERs resulting in a low potential of 259 mV at a current density of 10 $mAcm^{-2}$ in the alkaline medium. The significance of this research is that these composites show excellent OER over commercially used RuO_2. This group has expressed the OER process in the alkaline medium as follows,

$$* + OH^- \rightarrow HO^* + e^- \quad (9)$$

$$HO^* + OH^* \rightarrow O^* + e^- + H_2O \quad (10)$$

$$O^* + OH^- \rightarrow HOO^* + e^- \quad (11)$$

$$HOO^* + OH^- \rightarrow O_2{}^* + e^- + H_2O \quad (12)$$

$$O_2{}^* \rightarrow O_2 \quad (13)$$

here, * as denoted by the catalyst **(Equation 9–13)**. In this reaction process, HO^*, O^*, and HOO^* are adsorbed on the α-$Co(OH)_2$, and Co $(OH)_2$-GNS catalyst. They have confirmed by calculation that the overpotential of composite (0.28 V) is comparatively lower than that of pristine α-$Co(OH)_2$. From this study, it was concluded that this composite exhibit high electrocatalytic performance on OER by lowering the energy levels of intermediates and products [70].

3.3.3. Electrocatalytic CO_2 reduction reaction

CO_2 is the primary component of greenhouse gases, and its increasing severity has prompted numerous efforts exploring different ways to convert CO_2 to achieve sustainable development. CO_2 is gradually being reframed from a waste product to a plentiful renewable C_1resource. With a bond energy of up to 750 kJ/mol between its two bonds and two delocalized bonds, great thermodynamic stability, and poor electron affinity, the CO_2 molecule is notoriously difficult to reduce thermodynamically. In contrast, electrocatalytic CO2RR requires far lower temperatures and pressures than conventional thermochemical methods, and has emerged as a promising approach to convert CO_2 into a wide range of energy-related small molecules, like HCOOH, CO, CH_3OH, CH_4, C_2H_5OH, C_2H_4, involving a series of proton-coupled electron transfer reactions. However, when CO_2RR occurs in an aqueous electrolyte, the HER becomes a kinetically competitive process and should be avoided. Therefore, it is crucial to advance the catalysts that effectively accelerate CO_2 conversion with high selectivity, and minimal HER in aqueous conditions, together with high stability, natural abundance, and low cost. At this time, conversion of CO_2 into CO and HCOOH is more desirable. It is because the urgency of H_2 storage chemicals like HCOOH to benefit the fuel cells. In particular, HCOOH is a crucial intermediate in the synthesis of several compounds. HCOOH has also been used in CO_2 detection and capture and air separation [71,72]. Interestingly, compared to air, more oxygen vacancies can be produced during calcination under N_2. By using BDC as the organic linker, carbonization of MIL-68 yields the corn-like In_2O_{3-X}@C nanocomposite. The elevated electrical conductivity and catalytic activity can be attributed in part to the presence of numerous oxygen vacancies and amorphous carbon rods. DFT calculations show that In_2O_{3-X} has a strong propensity to spontaneously create HCOO* (*OCHO) intermediates, effectively boosting the energy barrier for the creation of *COOH intermediates, and so significantly improving the selectivity for HCOOH products **(**Fig. 8**(a-b))**, which gaining popularity as a liquid product with substantial economic benefits.

Furthermore, operando X-ray absorption spectroscopy (XAS) is used to investigate valence state changes that occur during the reaction. At 0.445 V **(**Fig. 8**c)**, essentially no HCOOH is formed because the in-valence state is below + 2. The FE_{HCOOH} content rises to about 85 % and the in-valence state approaches + 3 at a potential of 1.045 V. Further increasing the potential to 1.445 V reduces the FE_{HCOOH} to 51 %, and brings the valence state of in down to + 2.5. Fig. 8**d** depicts a hypothetical reaction process in which the catalyst undergoes a valence shift to In^0 during the initial reduction phase before reverting to In^{3+} following electron transfer to CO_2. Catalytic efficiency is limited by poor conductivity in the In-MOF (Me_2NH_2)[In(BCP)]2DMFn (V11) built from 5-(2,6-bis(4-carboxyphenyl)pyridin-4-yl) isophthalic acid (BCP), but this can be effectively improved by the introduction of carbon materials. The molecular structure and carbonization temperature of methylene blue (MB) allow it to integrate at the specified conditions. Above 250 °C, MB changes into carbon nanoparticles, whereas V11 retains structural stability up to 380 degrees Celsius, allowing V11 framework-loaded CPs to be formed in this temperature range **(**Fig. 8**e)**. By increasing the conductivity of the material and exposing more active sites, CPs produced from MB are utilized as promoters to ease charge and mass transfer during the reaction. This strategy's generality is highlighted by the fact that it may be used to other classical MOFs [75].

In summary, the electrochemical sector has paid growing attention to MOFs and their derivatives because of their outstanding properties. The electrocatalytic activity of MOFs has been shown to be greatly enhanced due to their ultrathin thickness, more accessible active sites, and reduced diffusion limitation. Despite their many advantages, studies of MOFs for electrochemical catalysis are still in their infancy, and much of the reported research has focused mostly on the OER, HER, and CO_2RR. The reaction mechanism can be better understood, allowing for the construction of far more efficient MOF-based electrocatalysts. Enhancing conductivities and electrochemical performance can be accomplished in a number of ways, including the creation of pure MOFs, the introduction of conductive substrates for MOFs, the hybridization of MOFs with other active materials, and high-temperature post-annealing [76].

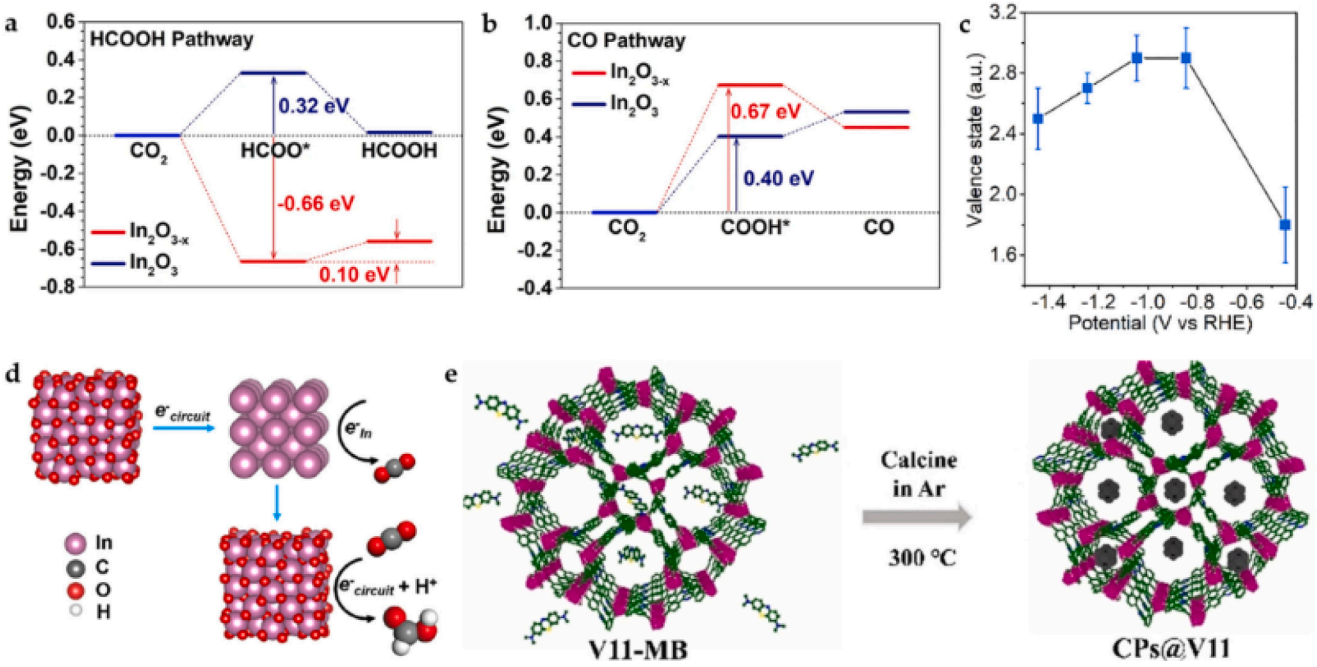

Fig. 8. Gibbs free energy profile for the CO_2conversion into(a) HCOOH, (b) CO @ In_2O_3 and In_2O_{3-x}. (c) Alterations in valence state in MIL-68-N_2upon various applied potentials. (d) The CO_2RR mechanism. Taken from [73], Copyright 2022, Springer Nature. (e) Representation of the synthesis strategy for CPs@V11. Taken from [74], Copyright 2021, Wiley-VCH.

3.4. Electrochemical energy storage

3.4.1. $_{Lithium}$-ion batteries

Since the introduction of batteries to the global market, the demand for batteries has expanded at a significant pace from small-scale production of portable devices including laptops, cameras, and mobile phones to electric vehicle manufacturing applications. Among those lithium-based energy storage devices, lithium-ion batteries (LIBs) have a considerable demand due to their unique characteristics of lightweight, small size, higher capacity, and high energy density compared to SCs, etc. Like SCs, the type of electrode material is a key factor that decides the electrochemical performance of lithium-ion batteries (LIBs). Thus, some shortcomings of LIBs hamper their commercial fabrication and applications. This is because of their low ion diffusion, poor conductivity, and low structural stability leading to a low rate of performance with a short lifetime. In this regard, several studies have been carried out in improving electrochemical performance with the cyclic stability of LIB devices [77].

Up to date, there are plenty of research studies involving various MOF-based composites in LIB applications. In this review, only the latest innovations are considered based on their results. Most research has developed MOF-based composites for anode materials in LIBs. Gao et al. synthesized Al-MOF/GR composite material as a negative electrode for LIBs using Al-MOF which is also known as MIL-53 having the chemical formula of Al(OH)[O_2C-C_6H_4-CO_2] and GR [77]. During the synthesis process, the composite formation is promoted by the electrostatic interaction between negatively charged GO and positively charged Al-MOF particles. By reacting with vitamin C, the GO in the composite was reduced to GR, forming the Al-MOF/GR structure. This group has found the band gap of Al-MOF/GR is relatively low compared to Al-MOF, which was 3.7 eV and 4.0 eV, respectively. The reduction of band gap after integrating with GR leads to producing more conductivity of this composite. This material exhibited a maximum specific capacity of 400 mAh/g at a current density of 100 mA/g after 100 cycles. Herein, the insertion and extraction of Li^+ ions mechanism involved in charge storage on this material. Later, in 2021, Han *et.al* used cobalt *meso*-tetrakis(4-carboxyphenyl) porphyrin (Co-TCPP MOF) and rGO to produce two-dimensional Co-TCPP MOF/ rGO nanosheets for LIB anodes [78]. The analysis of this material-based LIB, it showed a specific capacity of 1050 mAh/g at 100 mA/g after 100 cycles. The electrical conductivity of this composite increased with the incorporation of rGO, which blocks the growth of the Co-TCPP MOF particle assembly along the horizontal direction.

The examples discussed above all relate to MOF-based composites used to fabricate electrode materials for LIBs. In addition, these compounds can be developed for application as electrolytes in LIBs. In that sense, as a recent study, a highly conductive and stable solid polymer electrolyte (SPEs), Fe-MIL-88B modified with poly (ethylene oxide)-[PEO] was discovered by Han and his research team [79]. Basically, Fe-MOF acts as an inorganic filler to enhance the ionic conductivity of PEO-based SPEs. Apart from that, the functions of MOF in this composite electrolyte are to improve the mechanical properties and chemical stability of SPEs, control the fast transfer of Li^+ ions, and decrease the crystallization ratio of PEO. In this composite, the Lewis acid-base interaction between PEO and Fe-MOFs blocks the mobility of anions while accelerating the Li ions' movement. This group fabricated LIB using $LiFePO_4$, Li, and SPE as cathode, anode, and electrolyte, respectively. It has been concluded that this battery built with electrolyte exhibited higher cyclic stability and electric performance compared with other LIBs.

3.4.2. Supercapacitors

In energy storage applications, supercapacitors (SCs) which are also known as electrochemical capacitors have a high demand due to their unique properties of high specific capacitance, high power density, fast charge–discharge rate, and long cycle stability. The issue regarding SCs is their lower energy density. Nowadays, most researchers have found effective strategies to overcome the issues of these devices. As one example, developing hybrid SCs combining the other two types of SCs (Electrochemical double-layer capacitor and pseudo-capacitor) could be achieved battery-like high energy density. Typically, the type of electrode material and electrolyte are key factors that decide the chemical performance of the SCs. In that sense, several modifications including doping heteroatoms/ composing with electro-active components can be

applied to the electrode material to improve the electrochemical activity of the SC device [80–83].Among various electrode materials, MOF-composites and MOF-derived hybrid materials have gained great demand with the ability to tune the properties of the materials. In SC applications, MOFs can be applied in two different ways; (1) MOFs are used as direct electrode materials, (2) MOFs act as the template for developing other electroactive materials like metal oxide/sulfide/phosphides, and their composites through ion exchange/ one-step pyrolysis methods. The problem with the use of metal-based electrode material is that it decreases the active sites and surface area by demolishing the framework of MOFs. By introducing carbon nanotubes, conductive polymers (CPs), and GR into MOF, this issue can be overcome [84]. In this regard, various metals, CP, porous carbon, GR, and metal hydroxides/oxides are considered as additive materials used to enhance the conductivity and stability of MOFs. Besides that, there are several benefits that dopants bring to MOF-based composites, such as flexibility, high porosity, uniform pore structure, structural control, and enhanced electron transfer within the system [85].

As an example of metal-MOF-based composites used for ASCs, NiCo-MOF nanosheets as cathode electrode material was produced via the ultrasonication method by Wang and his research group [84]. In this experiment, Ni: Co ratio of 1:2 was used to prepare the composites of NiCo-MOF. They used this composite and activated carbon (AC) as the positive and negative electrodes in the fabrication of asymmetric SC (ASC).Later, in the same year, Tian et al. designed an ASC device using bimetallic MOF nanocomposites(PPNF@Co-Ni MOF) and KOH-activated carbon nanofibers doped with rGO (CNF-g) as cathode and anode, respectively(Fig. 9**a)** [86]Herein, they synthesized four different flower-like structured MOF-based electrode materials by varying the M of this composite (PPNF@M−Ni MOF; M = Zn, Cu, Fe, Co)(Fig. 9**h**). From those, PPNF@Co-Ni MOF was used to produce ASCs. The purpose of using preoxidized polyacrylonitrile nanofibers (PPNF) enhance the surface area and improve the cyclic stability and specific capacitance of this composite. Overall, this MOF-based composite material showed a higher specific capacitance (1096.2F/g) at 1A/g while showing 95 % of coulombic efficiency, and 85.5 % over 10 000 cycles at 10 A/g **(**Fig. 9**(b-f))**. Furthermore, the capacitance of this composite was tested by arranging the two composites in series for LED lighting **(**Fig. 9**g)**. In addition, this group elucidated the pseudocapacitive behavior of PPNF@Ni MOF and PPNF@Ni-Co MOF through redox reactions with OH^- ions from the electrolyte in **Equations (14) and (15)**, respectively.

Using alkaline electrolytes,

$$Ni_3(OH)_2(H_2O)_2(L)_2 + OH^- \leftrightarrow Ni_3(OH)_3(H_2O)(L)_2 + H_2O + e^- \quad (14)$$

$$Ni_{3-x}Co_x(OH)_3(OH)_2(H_2O)_2(L)_2 + OH^- \leftrightarrow Ni_{3-x}Co_x(OH)_3(H_2O)(L)_2 + H_2O + e^- \quad (15)$$

Regarding CP-based MOFs, Yue *et.al* synthesized electrode material combining porous structured polypyrrole (PPy) loaded MOF and carbon clothing to fabricate the flexible symmetric SC (SSC) [87]. In this study, PPy which is a CP was developed with MOFs to achieve high electrochemical performance as electrode material the function of CP in this composite is to provide extra capacitance and allow to transfer of more electrons leading to superior conductivity. In a most recent study, in 2022, Xie *et al.* examined the electrochemical performance of the SC using GO-attached MIL-101(Fe) as electrode material [88]. First, this material was tested using a three-electrode system. In this test, this

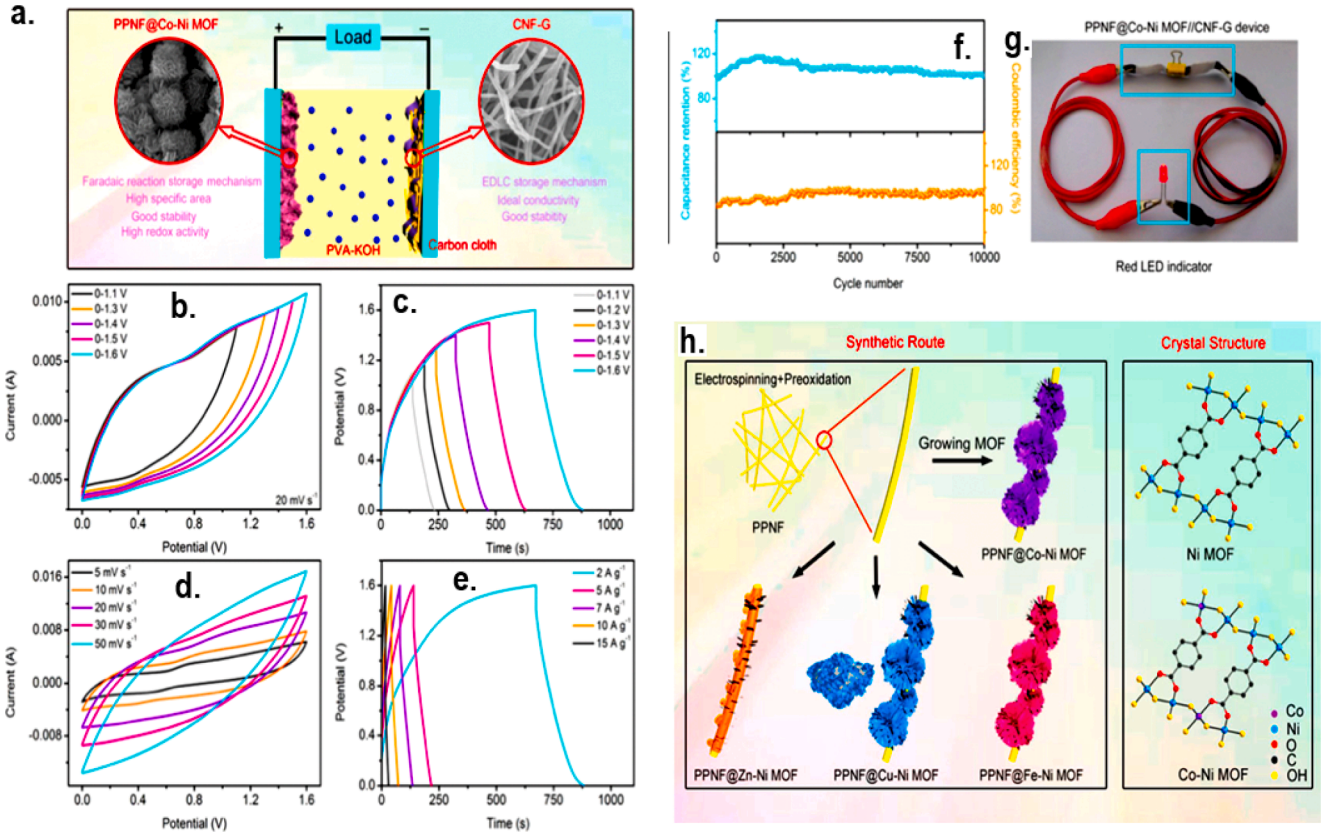

Fig. 9. (a) Schematic diagram of the asymmetrical supercapacitor, Electrochemical characterization of PPNF@Co-Ni MOF // CNF-G (b) CV analysis at 20 mV s^{-1} within different potential windows (c) GCD cycle analysis at 2 A/g within different potential windows, (d) CV analysis at various scan rate, (e) GCD cycle analysis various current densities, (f) Stability test, (g) demonstration of lighting a LED light using PPNF@Co-Ni MOF// CNF-G in series, (h) Synthetic method of four types of composites (PPNF@M−Ni, M = Zn, Cu, Fe, Co) and the crystal structures of Ni-MOF and Co-Ni MOF, adapted with permission [86], Copyright (2020), ACS Appl. Matter. Interfaces.

exhibited an excellent specific capacitance of 302.47F/g at 2 A/g and areal capacitance of 309.66 mF/cm^2 at 2 mA/cm^2 at a potential window of 0.9 V. The stability of this material in this system showed 80.01 % capacitance retention over 9000 cycles in the acidic electrolyte (3 M H_2SO_4). In CV analysis, they observed that GO@MIL-101 material exhibited two redox peaks within the potential range of 0.3 and 0.6 V which are responsible for charge storage. They defined two possible reactions which indicate two charge-storage mechanisms. They are redox reactions of Fe^{+3} ions on the composite **(Equation (16)** and adsorption–desorption reactions of H^+ ions on the surface of the GO@MIL-101 composite **(Equation (17)**. Consequently, this material was developed by composing with $Ti_3C_2T_x$ to use as an anode in ASC. The electrical performance of this device discussed in (Table 3**)** was relatively lower than that of the three-electrode system. Considering the symmetry, type of electrode, and electrolyte material, the most recent experimental results on the electrochemical performance of the MOF-composite-based SCs are summarized in the following (Table 3**)**. According to those results, it can be concluded that MOF-based composites are mainly used as cathode materials in ASCs.

Using acidic electrolytes,

$$MIL - FeOOH + H2O + e^- \leftrightarrow MIL - Fe(OH)_2 + 2H^+ \quad (16)$$

$$MIL - Fe^{3+} + H^+ + e^- \leftrightarrow H^+ - (MIL - Fe^{2+}) \quad (17)$$

These results indicate that MOF-based composites, due to their porosity and distinctive physico-chemical properties, can be recognized as viable electrode materials for Li-ion batteries and supercapacitors. Higher efficiency of Li-ion batteries and supercapacitors using MOF-based composites is within reach, but more development is necessary. This presents exciting new opportunities for the relevant scientific community.

3.5. Environmental remediation

3.5.1. Adsorption and degradation of organic dyes

With the rise of the industrial revolution, organic dyes were formed as hazardous products from the disposal of leftover dyes and the use of dyes commonly used in the textile industries. Due to their high toxicity and resistance to any harmful conditions, the accumulation of these types of pollutants in water has become a fatal problem these days. Various techniques including absorption, ultrafiltration, electrocoagulation, ozonation, and photodegradation [89–91]. Among those, light-assisted degradation and adsorption are effective strategies due to their low cost, high efficiency, and persistence. In wastewater treatment, methylene blue (MB), methyl orange, rhodamine-B (RhB), rhodamine-6G, malachite green, triphenylmethane, gentian violet, and reactive yellow-145 are some of the dyes which can be degraded by using MOF based composites. Herein, UiO-66 (Zr), MOF-5, ZIF-8, and MIL-125 (Ti) are some of the examples of MOF which are used in this application [90].

As one of the toxic organic dyes, RhB which has the chemical formula of $C_{28}H_{31}ClN_2O_3$, is a commonly found stain in wastewater. There are several studies related to RhB dye removal from water. Zang et al. fabricated a visible-light sensitive photocatalyst using iron terephthalate [MIL-53(Fe)] composed of graphene (GR) [89]. They have reported that this was the first innovation based on MOF-GR composite as a photocatalyst. For the synthesis, a solvothermal process was applied. Herein, the combination of reduced GR with MIL-53(Fe) allows transferring the photogenerated charge to an excited state, reducing the rate of recombination **(**Fig. 10**a)**. Regarding RhB degradation, GR/MIL-53(Fe)–H_2O_2 showed a better catalytic performance compared to that of MIL-53(Fe)–H_2O_2. To boost the photocatalytic activity, H_2O_2, which can stimulate photo-synergistic generation through the production of more hydroxyl radicals, was introduced to this system.

Recently, Ahmad Pour et.al discovered a photocatalyst of Ca/TiO_2/NH_2-MIL-125 for the degradation of RhB and MO ($C_{14}H_{14}N_3NaO_3S$) dyes under visible light irradiation [90]. Typically, dye removal has occurred through the adsorption mechanism of NH_2-MIL-125(Ti) **(**Fig. 10**b)**. The degradation mechanism of this composite starts with the transfer of electrons in TiO_2 from the valence band (VB) to the conduction band (CB) with the energy absorbed from sunlight, creating holes and electrons, respectively. Then, the excited electron in TiO_2, and charge carriers formed from the high conductive Ca surface are jumped into NH_2-MIL-125 to decrease the recombination of electron-hole pairs. Meanwhile, oxygen radicals are formed with the reaction of oxygen atoms with TiO_2**(Equation 18–23)**. The photocatalytic efficiency is improved through the oxidation of water reacting with holes in TiO_2. In summary, $^{\bullet}OH$, $^{\bullet}O_2$, and holes act as the charge carriers in this process. By introducing Ca into this compound, the rate of charge transfer between TiO_2 and NH_2-MIL-125 increases. The interaction between Ca and NH_2-MIL-125 promotes the photocatalytic role of TiO_2, efficiently degrading the dye pollutants of MO and RhB. The reactions involved in this process can be summarized as follows:

$$Ca/TiO_2/NH_2 - MIL - 125 \xrightarrow{UVlight(hv)} h^+ + e^- \quad (18)$$

$$O_2 + e^- \rightarrow \bullet O_2^- \quad (19)$$

$$Dyepollutant + \bullet O_2^- \rightarrow CO_2 + H_2O \quad (20)$$

$$Dyepollutant + h^+ \rightarrow CO_2 + H_2O \quad (21)$$

$$H_2O + h^+ \rightarrow \bullet OH + H^+ \quad (22)$$

$$Dyepollutant + \bullet OH. \rightarrow Degradedproducts + CO_2 + H_2O \quad (23)$$

In the practical application of this photocatalyst (Ca[30 %]/TiO_2/NH_2-MIL-125), some considerable factors can decide the large-scale

Table 3
Comparison of MOF-based composite as electrode material for supercapacitor applications.

Type of SC	Cathode	Anode	Electrolyte	Capacitance	Energy Density	Power Density	Stability	Ref.
SSC	p-PPy/Cu-CAT	p-PPy/Cu-CAT	3 M KCl	233 mF/cm^2	12μWh/ cm^2	1.5 mW/cm^2	85 % over 5000 cycles at 5 mA cm^{-2}	[70]
ASC	GO@MIL-101	GO@MIL-101/ $Ti_3C_2T_x$	3 M H_2SO_4	82.39F/g at 0.5 A/g, 93.99 mF/cm^2 at 2 mA/cm^2	20.68 Wh/kg	315 W/kg	89.6 % over 4000 cycles at 15 A/g	[71]
ASC	NiO@Ni-MOF/ NF	CNT	3 M KOH	144F/g at 1 A/g	39.2 Wh/kg	7000 W/kg	94 % over 3000 cycles at 10 A/g	[72]
ASC	NiCo-MOF	AC	2 M KOH	1202.1F/g at 1 A/g	49.4 Wh/kg	562.5 W/kg	76.7 % over 5000 cycles at 5 A/g	[67]
ASC	PPNF@Co-Ni MOF	CNF-g	PVA-KOH	1096.2F/g at 1A/g	93.6 Wh/kg	1600 W/kg	85.5 % over 10,000 cycles at 10 A/g	[69]
ASC	PPy-MOF	AC	3 M KOH	715.6F/g at 0.3 A/g	40.1 Wh/kg	1500.6 W/ kg	80 % over 10,000 cycles at 10 A/g	[73]
ASC	GA@UIO-66-NH2	$Ti_3C_2T_x$	1 M Na_2SO_4	651F/g at 2 A/g	73 Wh/kg	16000 W/kg	88 % over 10,000 cycles at 5.2 A/g	[74]

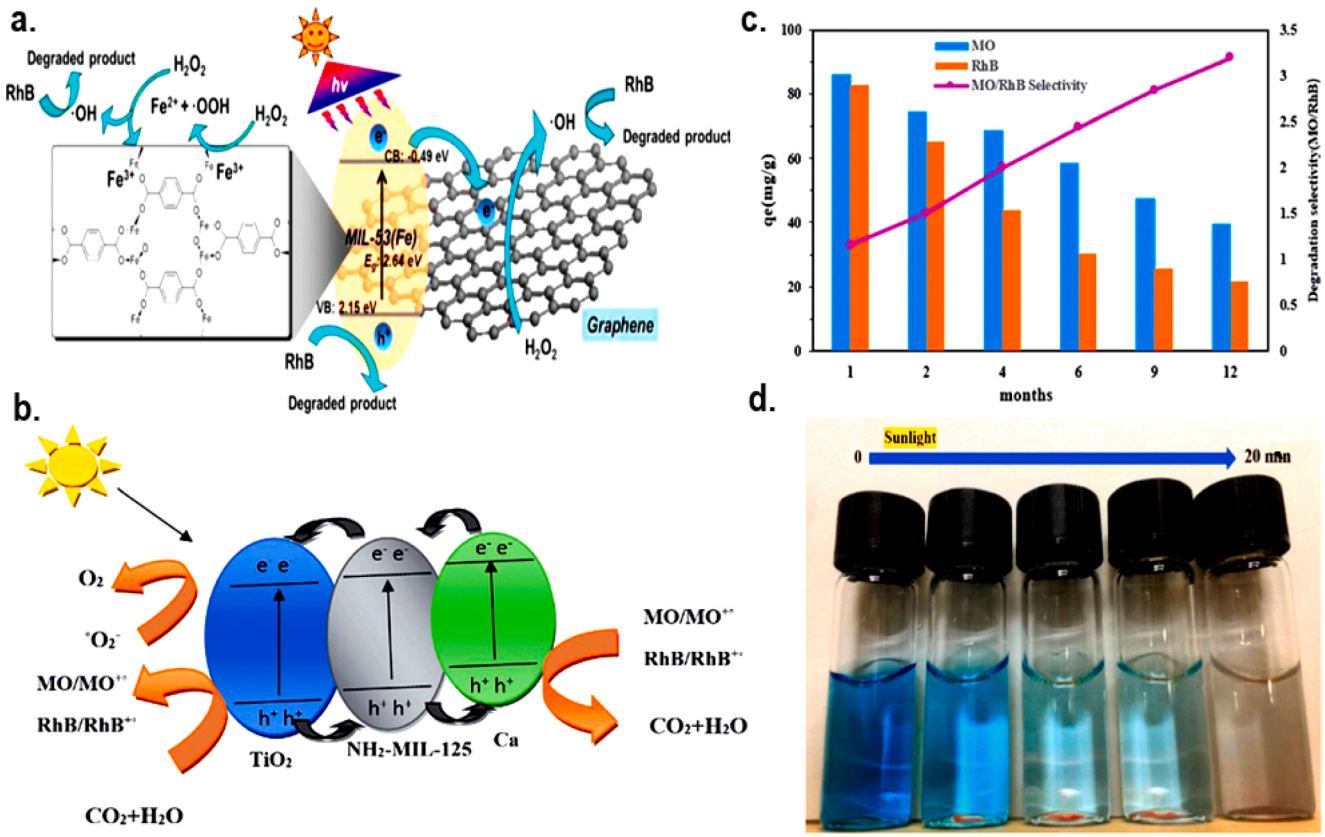

Fig. 10. (a) mechanism of RhB dye degradation through the catalysis of GR/MIL-53(Fe)–H_2O_2, adapted with permission [89], Copyright (2015), Ind. Eng. Chem. Res, (b) mechanism of RhB dye degradation through the catalysis of Ca[30 %]/TiO_2/NH_2-MIL-125, (c) the catalytic performance of Ca[30 %]/TiO_2/NH_2-MIL-125 for MO and RhB dye degradation, adapted with permission [90], Copyright (2020), RCS advances, (d) Color change representation of MB dye degradation reacted with MOF-5@rGO composite after 20 min, adapted with permission [91], Copyright (2020), Mater Sci Eng B.

production of these materials. They are reusability, stability, total organic carbon (TOC), and the water aging of photocatalytic nanoparticles. After data analysis, it was found that the degradation efficiency of RhB and MO in the first cycle showed 82.87 % and 86.22 %, respectively. After the 6 cycles, this value decreases to 69.18 % (RhB) and 73.29 % (MO). After the TOC analysis, this photocatalyst showed higher dye removal efficiency indicating TOC values of 39.47 % (RhB) and 43.02 % (MO). In addition, they examined the changes in catalytic efficiency for 12 months to determine the shelf life of this catalyst. The results confirmed that as the selectivity of Mo/RhB dye degradation increases, the removal efficiency decreases with time(Fig. 10**c)** [90].

A few months later, the same mechanism used in previous experiments was followed by this research group to synthesize MOF-5/reduced GO (MOF-5@rGO)composite for MB ($C_{16}H_{18}ClN_3S$) dye degradation [91]. Like other metallic materials, the photocatalytic performance of this composite was improved by introducing highly electroactive rGO, enhancing electron acceptance and avoiding the aggregation of electron-hole pairs through electron entrapping. In addition, the π-π interaction between the surface of the rGO and the dye molecules promotes dye absorption. Furthermore, the electrocatalytic activity of the composite improved with the increase of electron transfer rate due to the electrostatic interaction between the negatively charged oxygen groups of rGO and positively charged metal (Zn) ions of the MOF-5structure. This catalytic behavior was confirmed through the photoluminescence analysis. This group compared the percentage of dye degradation of MB, RhB, and MO after 20 min using MOF-5@rGO composite. Especially in the MB dye solution, this sample showed a 93 % of dye degradation, indicating a clear decrease in the color of the solution and the intensity of dye absorption after 20 min of observation time (Fig. 10**d**). Compared to this with the other two dyes, the dye degradation of MO and RhB in the presence of this composite was shown to be 92 % and 97 % in percentage, respectively. In summary, MOF-5@rGO showed excellent progress in various dye degradation applications over single materials.

3.5.2. Uptake, Separation, and cycloaddition of CO_2

As a negative impact of the industrial revolution, the amount of CO_2 in the atmosphere increased at an alarming rate. On average, CO_2 production from fuel combustion is estimated at approximately 30 gigatons per year. To date, the level of global atmospheric CO_2 concentration is projected around 400 ppm. In that condition, the CO_2 concentration is predicted to reach up to 570 ppm in 2100, which will bring more harmful effects to all life [92]. Due to this reason, it is necessary to find a way to control the amount of CO_2 gas level in the atmosphere. In this regard, capture, separation, and cycloaddition can be considered effective strategies that can be applied to control CO_2emissions from fossil fuel combustion in the industry. For this application, OF-based composites are suitable due to their desirable features of high porosity and large surface area with high active sites.

Several strategies have been developed to capture CO_2 including chemical/ physical absorption, cryogenic distillation, chemical/ physical adsorption, membrane permeation, and selective chemical looping [93]. Nowadays, organic alcohol amine solutions are commonly used in capturing CO_2atthe industrial level due to their attraction to the amine functional groups and CO_2 molecules. Thus, the usage of those compounds is limited by their high energy cost of redevelopment, corrosivity, and decomposition of amines. In that circumstance, MOF-based materials which can capture CO_2 by physical adsorption via Vander Waals interactions are developed. Depending on the pressure used for the experiment, the adsorption behavior of the MOF composite can be explained separately in low-pressure (including atmospheric pressure)

and high-pressure conditions. While many studies have revealed that MOFs with a high BET surface area exhibit high CO_2 adsorption capacity, this property does not act as a critical factor at low P [92]. Although it is quite challenging to use MOF to achieve the highest adsorption capacity at low partial pressure, it can be achieved by controlling the pore size, open metal sites (Lewis acids), Lewis bases, and other polar groups. In that sense, a combination of MOF with higher other porous materials such as activated carbon, and mesoporous SiO_2 leads to better performance by overcoming the drawbacks of pure MOFs. Chen et al. synthesized MIL-101@MCM-41 combining MIL-101(Cr) and mesoporous silica [94]. The CO2 adsorption capacity of this composite at 298 K and 1 bar showed 2.09 mmol/g which is 79 %. Higher than that of single MIL-101(Cr). The addition of MCM-41 to this composite increases the diffusion of CO_2 while sinking the mass transfer resistance which leads to an improved rate of absorption. The high stability of this compound was proved by reuse after 8 cycles without reducing the CO_2 adsorption capacity. In addition, Bolotov *et.al* developed aMOF-based composite, $Zn_2(tdc)_2dabco$, using thiophene-2,5-dicarboxylic acid (H_2tdc) and 1,4-diazabicyclooctane(dabco) to improve CO_2 capture efficiency of MOF [95].Herein, the phenyl group with thiophene in the composite leads to enhance CO_2 adsorption, and CO_2/N_2 selectivity without the contribution of metal ions. This is due to induced dipole interactions between CO_2 and sulfur elements in thiophene.

Apart from CO_2, the atmosphere consists of various gases like N_2, CH_4, and C_2H_2. Separating CO_2 from this gas system is quite a challenge. Thus, several mechanisms based on MOF compounds have been employed in the separation of CO_2 from gas mixtures. The principle behind those methods is to increase the selectivity of CO_2 adsorption in MOF composite over other gases. This can be achieved because of the variation in thermodynamic properties and filtering effects of pores in MOFs. The diameter of the pores of CO_2, N_2, and CH_4 are changed as 3.3, 3.64, and 3.76 °A, respectively. Based on these values, CO_2 can easily separate from N_2 and CH_4 gases due to its lower pore diameter. CO_2 has a higher tendency to occupy active sites on MOFs compared to non-polar compounds of N_2 and CH_4.The issue related to the use of MOFs are affinity to water vapor and trace acid limited CO_2 absorption and separation. These drawbacks can be overcome by developing MOFs by attaching hydrophobic functional groups [92].

With the adsorption and separation of CO_2, it can be treated via the process of biochemical, thermochemical, photochemical, or electrochemical converting this gas into value-added eco-friendly outcomes. In these reactions, methanol, polyol, dimethyl ether, and cyclic carbonate (CC) are obtained as intermediates, and further treatment leads to the formation of aromatic substances and liquid fuel as final products. In this review, the formation of cyclic carbonate products through the cycloaddition of CO_2 with an epoxide in the presence of a catalyst has been discussed as one of the effective methods of controlling CO_2 levels. In these reactions, MOF-based composites act as an efficient candidate for heterogeneous catalysis. Considering the mechanism, four steps are involved in this reaction. They are (i) the adsorption of epoxide, (ii) the epoxide ring-opening, (iii) the CO_2 addition, and (iv) the closing of the ring with the formation of CC [96]. As an example, Liu et.al synthesized MIL-101-IMBr composite by modifying MOF with imidazolium-based ionic liquids [97].In this study, under mild and co-catalyst-free conditions, a higher catalytic activity for the cycloaddition of CO_2 with epoxides was observed from this composite. It has been calculated that the conversion of propylene oxide and selectivity of CC resulted in 95.8 % and 97.6 %, respectively. This catalyst has a higher stability, showing stable performance after 5 cycles. In summary, porous MOF composite materials are a great innovation as catalysts in controlling CO_2levels in the global atmosphere.

3.6. Other applications of MOF-based composites

In addition to energy, environment, and catalytic functions, the uses of MOF-based composites have expanded in a wide range of applications such as photoluminescence (PL), photosensitizing, uptake, and destruction of chemical warfare agents (ex: sulfur mustard and soman), CO_2 photoconversion, Perovskite solar cells, ratiometric optical temperature sensing, etc. In this section, only a few selected applications based on recent studies are briefly reviewed. For photophysical and photochemical purposes, MOF-based materials can be arranged as chromophores that can be applied as antennas in sensors and photocatalysts. The integrated properties of MOFs, including light harvesting capability, in-system energy transfer mechanism, and photocatalysis contribute to sensing improvements. Herein, a high degree of chromophore arrangement in the MOF-based structure leads to capturing more photons to harvest more lights [98]. The incorporation of MOF with quantum dots (QDs) can be considered an efficient way to enhance the absorption area of the MOF. It has been found that QDs have high light-emitting capacity due to their narrow band-edge PL with high emission Q yield and broad absorption range. It has been estimated that 50 % more photons can be absorbed than using single MOFs. In this regard, Kumagai and his group have done several studies to illustrate the light-harvesting property of QD-MOF composites using different types of MOFs. In 2019, this group observed the stability of the QDs and surface modifying ability of zeolite-based MOF through the synthesis of QD/ZIF-8 composite. In this structure, CdSe/CdS core/shell QDs were completely covered with ZIF-8 crystallites, which shows 40 % of PL [99].In their most recent research, two types of QD-IRMOF-3 composite were synthesized to determine the best structure for energy transfer efficiency **(**Fig. 11**a)** [100].The core–shell structure, constructed by covering the acceptor material of QDs with the donor without any linkages has been confirmed as an ideal candidate for energy transport. In this study, they discovered that the energy transfer efficiency of the QD-supported IRMOF-3 composite was 11 times lower than that of the QD-IRMOF-3 core/shell composite. When comparing the PL intensity of the QDs when excited at the absorption maximum of the IRMOF-3 shell, it was twice than that of the pristine QDs efficiency **(**Fig. 11**b).**In addition, the halide perovskite QDs@MOF composite was designed by embedding QDs on the luminescent MOF by Bhattacharyya et al to demonstrate the optoelectrical properties [101]. Herein, they confirmed that Pb^{II}-stabilized AMOF composites exhibit high luminescence characteristics that can be applied in various specialized applications. As another way to improve the overall absorption of MOF, the insertion of molecular sensitizers into the pores of MOF can be introduced. In summary, the PL of MOF can be improved through the new design of the organic linkers, integration of light harvesting gust materials like QDs, sensitizers, and so on [98–100].

One of the inspiring applications of MOF-based composites is the degradation of chemical warfare agents (CWAs) which are extremely toxic substances, used to kill or injure living beings. Simply, these agents are used as chemical weapons for military attacks. To date, several strategies have been discovered to detoxify those chemical compounds. In previous works, corrosive agent of sulfur mustard (HD), and neurotoxic agent of soman (GD) such as DS2-Decontamination Solution-2, sodium hydroxide, and calcium hypochlorite were decontaminated by using strong and alkaline solutions (ex: hypochlorite salts). Although these disinfectant solutions are capable of rapidly decontaminating CWA, their corrosive nature can cause severe damage more than that. Later, less harmful nano-oxides were discovered. The problem with them is that they require more quantity to disinfect. In that regard, it is necessary to find eco-friendly, multifunctional, efficient decontaminants which can be applied to any type of CWA [102]. Typically, Zr_6 metal centers have been found to be capable of hydrolyzing corrosive agents, and MOF synthesis by coupling the metal with photocatalytic/syringic aminated ligands leads to the oxidation of corrosive mustard agents. The powder form of the MOF-composites was found to be highly reactive in a short time (1 min) in decomposing CWAs. Consequently, this was developed to fabricate MOF-functionalized fibers used in military uniforms, filtration units, tents, etc. Thus, there were some limitations in the synthesis process such as control of the packing and uniformity of the

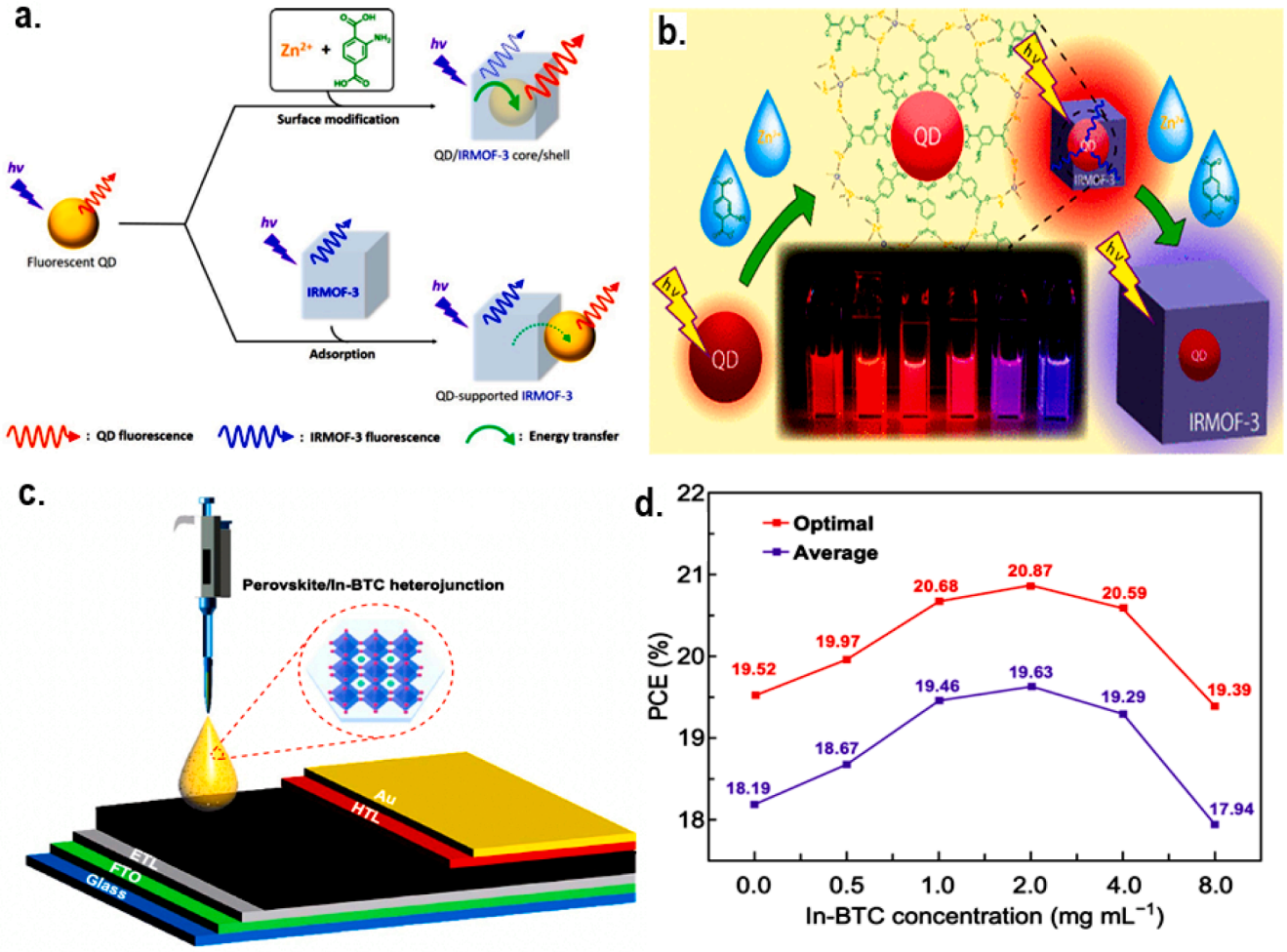

Fig. 11. (a) Schematic diagrams of two types of QD@MOF composites; QD/IRMOF-3 core/shell composite and QD supported IRMOF-3, (b)The color variation of QDs and QD/IRMOF-3 composites under UV irradiation, adapted with permission [100], Copyright (2021), Chemistry of materials, (c) Schematic representation of fabrication of perovskite solar cells using MOF/perovskite heterojunction composites, (d) Variation of Power conversion efficiency with the changes of In-BTC concentration in perovskite solar cells, adapted with permission [104], Copyright (2020), Nano-Micro Letters.

material, and the deterioration of the fabric under a harsh environment. To overcome these issues, MOFs can be deposited on pretreated fibers with metal oxide (MO). The ability to enhance MOF growth by combining with metal oxides has been useful in making MOF-based composites. There are possible mechanisms such as direct nucleation, and conversion of MO into MOF through linker diffusion. For an instance, MIL-96 and MIL-53-NH_2 were prepared by converting atomic layer deposited (ALD) Al_2O_3 coated fibers through the diffusion of linker into MO film at optimum conditions (15 bar and 110 °C). Further, Al-PMOF and ALD Al_2O_3 were synthesized by using porphyrin linkers. In this regard, Barton *et al.* synthesized fibrous MOF composites to capture or degrade CWAs and simulants. In this study, they observed the activity of MOF-525 growth on MO-coated polypropylene (PP) fibers to degrade CWA (ex: dimethyl-4-nitrophenyl phosphate) [103].Herein, heterogeneous nucleation of the polycrystalline structure of MOFs can be promoted by metal oxides such as Al_2O_3, ZnO, ZrO, HfO_2, and TiO_2. Based on the type of MO, the nucleation of MOFs changes. The higher growth of MOF leads to a higher rate of DMNP degradation. In this study, this group compared the degradation performance of PP/TiO_2/ MOF-525 and PP/Al_2O_3/MOF-525. From those, they found that PP/TiO_2/MOF-525 showed higher growth performance resulting in higher DMNP degradation.

In addition, MOF-based composites are also very applicable in fabricating perovskite solar cells (PSCs). As a thin film photovoltaic device, PSCs are more popular because of their facile synthesis, low cost, and high energy conversion efficiency. Typically, the creation, separation, transfer, and recombination of electron-hole pairs are the main factors that affect the photoelectric efficiency of PSCs. Considering the unique properties of high capacity and long-lifecycles, MOF-based composites have been widely used in the fabrication of PSCs [105]. Recently, Zhou et.al synthesized light-harvesting layers of MOF/perovskite heterojunction composites by combining microporous indium (III)-based MOF $(In_{12}O(OH)_{16}(H_2O)_5(btc)_6]_n$ [In-BTC] nanocrystals with perovskite films with the purpose of improving stability and efficiency of PSCs (Fig. 11**c**) [104]. In that case, the optimum composition of perovskite/In-BTC heterojunction was examined by increasing the In-BTC concentration. Then, they found that this composite achieved 20.87 % of optimal power conversion efficiency (PCE)at 2.0 mg/mL and 0.79 fill factors higher than that of pristine devices which was 19.52 % and 0.76, respectively (Fig. 11**d**). In this composite, In-BTC act as an additive that contributes to improving the crystallinity and morphological features of the perovskite films with the reduction of their defects and grain boundaries. This group observed that 80 % of initial PCE was maintained even inan ultra-humid atmosphere for 12 days without any coating, indicating the high stability of In-BTC-based PSCs.

4. Summary and perspectives

Based on the previously discussed research works on MOF-based composites, it can be confirmed that the structures and properties of

these materials can be modified based on the requirement of the applications in which they are applied. Herein, the best performance in many activities could be achieved because of their flexible, tunable morphological characteristics like high surface area, porosity, etc. Particularly, MOF-based compounds are highly beneficial as heterogeneous catalysts in various applications such as ODS, hydroxylation, oxidation of organic compounds, CO_2 reduction, and water oxidation considering the most common properties such as high recyclability, chemical stability, and environmental sustainability. When examining the past records, it is noticeable fact that research related to the characterization of MOF composites is relatively less compared with that of pure MOF materials.

In this review, the recent development of MOF-based composites in catalytic, energy, and environmental applications along with changes in their structural, properties are clearly discussed. With the rise of the industrial revolution, the rate of air and water pollution rises to a menacing level due to the emission of waste from industrial-scale production. In that sense, these composites can be used to control the hazardous effects in different ways. Many research studies have found that different types of MOF-composed materials have achieved the best performance through different mechanisms. Currently, there is a significant achievement obtained in understanding the behavior of MOF-based composites based on their desired application. Thus, when those innovations are brought from the laboratory scale to real-world practices, there are still some drawbacks in the performance and practical use of these materials. For example, the low yield of the product obtained, and the uneven arrangement of the MOF and guest elements in the structure caused some challenges while synthesizing those materials. Also, controlling the thermodynamics and kinetics of composites during reactions is a difficult task and this will affect the meeting of the needs of real applications. These are some challenges in the fabrication process of MOF composites. With the introduction of new techniques for synthesis, it will accelerate the discovery of stable, effective structures that achieve desired properties and potential performances.

Certain research questions in specific applications are still unpredictable and more research should be carried out to find a way to overcome the related problems. For an instance, it is difficult to separate CO_2 and C_2H_2 gas molecules in gas separation applications because of their similar size. Although this research question remains unsolved, associated investigations are steadily growing with novel suggestions. It has been noted that there was a lack of research on developing MOF-based composite on perovskite solar cells. In that sense, the use of MOF-based composites can pave the way for new future-oriented research avenues through the development of new functional materials and derivatives of MOF. Finally, it is hoped that this review will support new researchers to explore more innovations in this field.

Declaration of Competing Interest

The authors declare that they have no known competing financial interests or personal relationships that could have appeared to influence the work reported in this paper.

Data availability

No data was used for the research described in the article.

References

[1] Q. Zhang, H. Yang, T. Zhou, X. Chen, W. Li, H. Pang, Adv. Sci. 9 (2022) 2204141.
[2] O.M. Yaghi, G. Li, H. Li, Nature 378 (1995) 703–706.
[3] H.J. Xu, P.Y. Hu, J. Clean. Prod. (2023) 136253.
[4] H.C. Zhou, R.L. Jeffrey, M.Y. Omar, Chem. Rev. 112 (2012) 673–674.
[5] L. Chen, Q. Xu, Matter 1 (2019) 57–89.
[6] H. Li, M. Eddaoudi, M. O'Keeffe, O.M. Yaghi, Nature 402 (1999) 276–279.
[7] L. Feng, K.-Y. Wang, J. Willman, H.-C. Zhou, ACS Cent. Sci. 6 (2020) 359–367.
[8] L. Feng, K.-Y. Wang, J. Powell, H.-C. Zhou, Matter 1 (2019) 801–824.
[9] N. Yanai, S. Granick, Angew. Chem. 124 (2012) 5736–5739.
[10] S. Zhang, Y. Zhang, F. Baig, T.-F. Liu, Cryst. Growth Des. 21 (2021) 3100–3122.
[11] W. Yao, J. Chen, Y. Wang, R. Fang, Z. Qin, X. Yang, L. Chen, Y. Li, Angew. Chem. 133 (2021) 23922–23927.
[12] W. Yao, A. Hu, J. Ding, N. Wang, Z. Qin, X. Yang, K. Shen, L. Chen, Y. Li, Adv. Mater. (2023) 2301894.
[13] L. Chen, R. Luque, Y. Li, Chem. Soc. Rev. 46 (2017) 4614–4630.
[14] C. Xu, R. Fang, R. Luque, L. Chen, Y. Li, Coord. Chem. Rev. 388 (2019) 268–292.
[15] L. Chen, N. Tsumori, Q. Xu, Sci. China Chem. 63 (2020) 1601–1607.
[16] N. Tsumori, L. Chen, Q. Wang, Q.-L. Zhu, M. Kitta, Q. Xu, Chem 4 (2018) 845–856.
[17] A.E. Baumann, D.A. Burns, B. Liu, V.S. Thoi, Communications Chemistry 2 (2019) 86.
[18] N.C. Burtch, H. Jasuja, K.S. Walton, Chem. Rev. 114 (2014) 10575–10612.
[19] S. Yuan, L. Feng, K. Wang, J. Pang, M. Bosch, C. Lollar, Y. Sun, J. Qin, X. Yang, P. Zhang, Adv. Mater. 30 (2018) 1704303.
[20] fish 0,punct]">I.J. Kang, N.A. Khan, E. Haque, S.H. Jhung, Chemistry–A, European Journal 17 (2011) 6437–6442.
[21] J.H. Cavka, S. Jakobsen, U. Olsbye, N. Guillou, C. Lamberti, S. Bordiga, K. P. Lillerud, J. Am. Chem. Soc. 130 (2008) 13850–13851.
[22] H.-L. Jiang, T.A. Makal, H.-C. Zhou, Coord. Chem. Rev. 257 (2013) 2232–2249.
[23] S. Li, F. Huo, Nanoscale 7 (2015) 7482–7501.
[24] M.C. De Koning, K. Ma, M. Van Grol, I. Iordanov, M.J. Kruijne, K.B. Idrees, H. Xie, T. Islamoglu, R.P. Bross, O.K. Farha, Chem. Mater. 34 (2022) 1269–1277.
[25] G.W. Peterson, D.T. Lee, H.F. Barton, T.H. Epps III, G.N. Parsons, Nat. Rev. Mater. 6 (2021) 605–621.
[26] V. Unnikrishnan, O. Zabihi, M. Ahmadi, Q. Li, P. Blanchard, A. Kiziltas, M. Naebe, J. Mater. Chem. A 9 (2021) 4348–4378.
[27] I. Ahmed, S.H. Jhung, Mater. Today 17 (2014) 136–146.
[28] S. Luo, Z. Zeng, G. Zeng, Z. Liu, R. Xiao, M. Chen, L. Tang, W. Tang, C. Lai, M. Cheng, ACS Appl. Mater. Interfaces 11 (2019) 32579–32598.
[29] A. Bavykina, N. Kolobov, I.S. Khan, J.A. Bau, A. Ramirez, J. Gascon, Chem. Rev. 120 (2020) 8468–8535.
[30] C. Dai, A. Zhang, C. Song, X. Guo, Adv. Catal. (2018) 75–115.
[31] Y. Liu, C. Tang, M. Cheng, M. Chen, S. Chen, L. Lei, Y. Chen, H. Yi, Y. Fu, L. Li, ACS Catal. 11 (2021) 13374–13396.
[32] Y. Xue, G. Zhao, R. Yang, F. Chu, J. Chen, L. Wang, X. Huang, Nanoscale 13 (2021) 3911–3936.
[33] P. Cancino, A. Vega, A. Santiago-Portillo, S. Navalon, M. Alvaro, P. Aguirre, E. Spodine, H. García, Cat. Sci. Technol. 6 (2016) 3727–3736.
[34] G. Li, S. Zhao, Y. Zhang, Z. Tang, Adv. Mater. 30 (2018) 1800702.
[35] F. Boshagh, M. Rahmani, K. Rostami, M. Yousefifar, Energy Fuel 36 (2021) 98–132.
[36] S.S. Bello, C. Wang, M. Zhang, H. Gao, Z. Han, L. Shi, F. Su, G. Xu, Energy Fuel 35 (2021) 10998–11016.
[37] S. Kumar, V.C. Srivastava, S.M. Nanoti, Sep. Purif. Rev. 46 (2017) 319–347.
[38] M.A. Dinamarca, C. Ibacache-Quiroga, P. Baeza, S. Galvez, M. Villarroel, P. Olivero, J. Ojeda, Bioresour. Technol. 101 (2010) 2375–2378.
[39] I. Ahmed, S.H. Jhung, J. Hazard. Mater. 301 (2016) 259–276.
[40] Y. Wu, L. Wang, J. Phys. Chem. C 126 (2022) 18822–18832.
[41] M.T. Timko, A.F. Ghoniem, W.H. Green, J. Supercrit. Fluids 96 (2015) 114–123.
[42] K. Rychlewska, K. Konieczny, M. Bodzek, Archives of Environmental Protection 41 (2015) 3–11.
[43] A. Tanimu, G. Tanimu, S.A. Ganiyu, Y. Gambo, H. Alasiri, K. Alhooshani, Energy Fuel 36 (2022) 3394–3419.
[44] Z.-J. Lin, H.-Q. Zheng, J. Chen, W.-E. Zhuang, Y.-X. Lin, J.-W. Su, Y.-B. Huang, R. Cao, Inorg. Chem. 57 (2018) 13009–13019.
[45] M.A. Betiha, A.M. Rabie, H.S. Ahmed, A.A. Abdelrahman, M.F. El-Shahat, Egypt. J. Pet. 27 (2018) 715–730.
[46] M.A. Rezvani, A.F. Shojaie, M.H. Loghmani, Catal. Commun. 25 (2012) 36–40.
[47] S. Ribeiro, C.M. Granadeiro, P. Silva, F.A.A. Paz, F.F. de Biani, L. Cunha-Silva, S. S. Balula, Cat. Sci. Technol. 3 (2013) 2404–2414.
[48] X.-S. Wang, Y.-B. Huang, Z.-J. Lin, R. Cao, Dalton Trans. 43 (2014) (1958) 11950–11951.
[49] S.W. Li, R.M. Gao, R.L. Zhang, J.S. Zhao, Fuel 184 (2016) 18–27.
[50] Y.-L. Peng, J. Liu, H.-F. Zhang, D. Luo, D. Li, Inorg. Chem. Front. 5 (2018) 1563–1569.
[51] P. Wei, Y. Yang, W. Li, G. Li, Fuel 274 (2020) 117834.
[52] W. Sun, L. Gao, G. Zheng, Chem. Commun. 55 (2019) 8915–8918.
[53] A.D. Salazar-Aguilar, G. Vega, J.A. Casas, S.M. Vega-Díaz, F. Tristan, D. Meneses-Rodríguez, M. Belmonte, A. Quintanilla, Catalysts 10 (2020) 172.
[54] B.l. Xiang, L. Fu, Y. Li, Y. Liu, ChemistrySelect 4 (2019) 13638–13645.
[55] G.-J. Chen, J.-S. Wang, F.-Z. Jin, M.-Y. Liu, C.-W. Zhao, Y.-A. Li, Y.-B. Dong, Inorg. Chem. 55 (2016) 3058–3064.
[56] A. Dhakshinamoorthy, E. Montero Lanzuela, S. Navalon, H. Garcia, Catalysts 11 (2021) 95.
[57] G. Chen, S. Wu, H. Liu, H. Jiang, Y. Li, Green Chem. 15 (2013) 230–235.
[58] A. Paul, L.M. Martins, A. Karmakar, M.L. Kuznetsov, A.S. Novikov, M.F.C.G. da Silva, A.J. Pombeiro, J. Catal. 385 (2020) 324–337.
[59] J. Tong, W. Wang, L. Su, Q. Li, F. Liu, W. Ma, Z. Lei, L. Bo, Cat. Sci. Technol. 7 (2017) 222–230.
[60] Z. Han, Y. Fu, Y. Zhang, X. Zhang, X. Meng, Z. Zhou, Z. Su, Dalton Trans. 50 (2021) 3186–3192.
[61] X.-M. Cheng, P. Wang, S.-Q. Wang, J. Zhao, W.-Y. Sun, ACS Appl. Mater. Interfaces 14 (2022) 32350–32359.
[62] L. Shi, T. Wang, H. Zhang, K. Chang, J. Ye, Adv. Funct. Mater. 25 (2015) 5360–5367.
[63] S. Liu, F. Chen, S. Li, X. Peng, Y. Xiong, Appl Catal B 211 (2017) 1–10.

[64] G. Xu, H. Zhang, J. Wei, H.-X. Zhang, X. Wu, Y. Li, C. Li, J. Zhang, J. Ye, ACS Nano 12 (2018) 5333–5340.
[65] Y. Wang, L. Guo, Y. Zeng, H. Guo, S. Wan, M. Ou, S. Zhang, Q. Zhong, ACS Appl. Mater. Interfaces 11 (2019) 30673–30681.
[66] L. Zhao, Z. Zhao, Y. Li, X. Chu, Z. Li, Y. Qu, L. Bai, L. Jing, Nanoscale 12 (2020) 10010–10018.
[67] X. Zou, Y. Zhang, Chem. Soc. Rev. 44 (2015) 5148–5180.
[68] M.D. Makhafola, K.E. Ramohlola, T.C. Maponya, T.R. Somo, E.I. Iwuoha, K. Makgopa, M.J. Hato, K.M. Molapo, K.D. Modibane, Int. J. Electrochem. Sci. 15 (2020) 4884–4899.
[69] K. Jayaramulu, S. Mukherjee, D.M. Morales, D.P. Dubal, A.K. Nanjundan, A. Schneemann, J. Masa, S. Kment, W. Schuhmann, M. Otyepka, Chem. Rev. 122 (2022) 17241–17338.
[70] M. Huang, W. Liu, L. Wang, J. Liu, G. Chen, W. You, J. Zhang, L. Yuan, X. Zhang, R. Che, Nano Res. 13 (2020) 810–817.
[71] F. Li, G.H. Gu, C. Choi, P. Kolla, S. Hong, T.-S. Wu, Y.-L. Soo, J. Masa, S. Mukerjee, Y. Jung, Appl Catal B 277 (2020) 119241.
[72] L. Xue, C. Zhang, T. Shi, S. Liu, H. Zhang, M. Sun, F. Liu, Y. Liu, Y. Wang, X. Gu, Chem. Eng. J. 452 (2023) 139701.
[73] C. Qiu, K. Qian, J. Yu, M. Sun, S. Cao, J. Gao, R. Yu, L. Fang, Y. Yao, X. Lu, Nano-Micro Letters 14 (2022) 167.
[74] Z.H. Zhu, B.H. Zhao, S.L. Hou, X.L. Jiang, Z.L. Liang, B. Zhang, B. Zhao, Angew. Chem. 133 (2021) 23582–23590.
[75] R. Ye, Y. Tong, D. Feng, P. Chen, J. Mater. Chem. A 11 (2023) 4691–4702.
[76] Y. Lei, Z. Wang, A. Bao, X. Tang, X. Huang, H. Yi, S. Zhao, T. Sun, J. Wang, F. Gao, Chem. Eng. J. 453 (2023) 139663.
[77] C. Gao, P. Wang, Z. Wang, S.K. Kær, Y. Zhang, Y. Yue, Nano Energy 65 (2019) 104032.
[78] Y. Han, Z. Liu, F. Zheng, Y. Bai, Z. Zhang, X. Li, W. Xiong, J. Zhang, A. Yuan, J. Alloy. Compd. 881 (2021) 160531.
[79] D. Han, Z. Zhao, Z. Xu, H. Wang, Z. He, H. Wang, J. Shi, L. Zheng, ACS Applied Energy Materials 5 (2022) 8973–8981.
[80] B. Pal, S. Yang, S. Ramesh, V. Thangadurai, R. Jose, Nanoscale Advances 1 (2019) 3807–3835.
[81] H. Liu, X. Liu, S. Wang, H.-K. Liu, L. Li, Energy Storage Mater. 28 (2020) 122–145.
[82] R. Reece, C. Lekakou, P.A. Smith, ACS Appl. Mater. Interfaces 12 (2020) 25683–25692.
[83] P. Forouzandeh, V. Kumaravel, S.C. Pillai, Catalysts 10 (2020) 969.
[84] Y. Wang, Y. Liu, H. Wang, W. Liu, Y. Li, J. Zhang, H. Hou, J. Yang, ACS Applied Energy Materials 2 (2019) 2063–2071.
[85] Z. Cao, R. Momen, S. Tao, D. Xiong, Z. Song, X. Xiao, W. Deng, H. Hou, S. Yasar, S. Altin, Nano-Micro Letters 14 (2022) 181.
[86] D. Tian, N. Song, M. Zhong, X. Lu, C. Wang, ACS Appl. Mater. Interfaces 12 (2019) 1280–1291.
[87] T. Yue, R. Hou, X. Liu, K. Qi, Z. Chen, Y. Qiu, X. Guo, B.Y. Xia, ACS Applied Energy Materials 3 (2020) (1928) 11920–11921.
[88] J. Xie, R. Ma, H. Fang, H. Shi, D. Liu, Cryst. Growth Des. 22 (2022) 2997–3006.
[89] C. Zhang, L. Ai, J. Jiang, Ind. Eng. Chem. Res. 54 (2015) 153–163.
[90] N. Ahmadpour, M.H. Sayadi, S. Homaeigohar, RSC Adv. 10 (2020) 29808–29820.
[91] Q.V. Thi, M.S. Tamboli, Q.T.H. Ta, G.B. Kolekar, D. Sohn, Mater. Sci. Eng. B 261 (2020) 114678.
[92] Z. Li, P. Liu, C. Ou, X. Dong, ACS Sustain. Chem. Eng. 8 (2020) 15378–15404.
[93] P. Madejski, K. Chmiel, N. Subramanian, T. Kuś, Energies 15 (2022) 887.
[94] C. Chen, N. Feng, Q. Guo, Z. Li, X. Li, J. Ding, L. Wang, H. Wan, G. Guan, J. Colloid Interface Sci. 513 (2018) 891–902.
[95] V.A. Bolotov, K.A. Kovalenko, D.G. Samsonenko, X. Han, X. Zhang, G.L. Smith, L. J. McCormick, S.J. Teat, S. Yang, M.J. Lennox, Inorg. Chem. 57 (2018) 5074–5082.
[96] S.G. Musa, Z.M. Aljunid Merican, O. Akbarzadeh, Polymers 13 (2021) 3905.
[97] D. Liu, G. Li, H. Liu, Appl. Surf. Sci. 428 (2018) 218–225.
[98] E.A. Dolgopolova, A.M. Rice, C.R. Martin, N.B. Shustova, Chem. Soc. Rev. 47 (2018) 4710–4728.
[99] K. Kumagai, T. Uematsu, T. Torimoto, S. Kuwabata, CrstEngComm 21 (2019) 5568–5577.
[100] K. Kumagai, T. Uematsu, T. Torimoto, S. Kuwabata, Chem. Mater. 33 (2020) 1607–1617.
[101] S. Bhattacharyya, D. Rambabu, T.K. Maji, J. Mater. Chem. A 7 (2019) 21106–21111.
[102] J. Yu, Q. Gao, L. Zhang, Y. Zhou, Y. Zhong, J. Yin, Y. Zhou, F. Tao, Dalton Trans. 49 (2020) 8122–8135.
[103] H.F. Barton, A.K. Davis, G.N. Parsons, ACS Appl. Mater. Interfaces 12 (2020) 14690–14701.
[104] X. Zhou, L. Qiu, R. Fan, J. Zhang, S. Hao, Y. Yang, Nano-Micro Letters 12 (2020) 1–11.
[105] M. Shen, Y. Zhang, H. Xu, H. Ma, Iscience 24 (2021) 103464–103508.

Ram K. Gupta is an Associate Professor at Pittsburg State University. Dr. Gupta's research focuses on nano magnetism, nanomaterials, green energy production and storage using conducting polymers and composites, sensors, electrocatalysts for fuel cells, optoelectronics and photovoltaics devices, organic-inorganic hetero-junctions for sensors, bio-based polymers, biocompatible nanofibers for tissue regeneration, scaffold and antibacterial applications, and biodegradable metallic implants. Dr. Gupta has published over 250peer-reviewed articles, made over 350 national/international/regional presentations, chaired many sessions at national/international meetings, and edited/wrote several books/chapters for the American Chemical Society, the Royal Society of Chemistry, CRC, Elsevier, Springer, and Wiley. He has received several million dollars for research and educational activities from external agencies. He is a serving Associate Editor, Guest Editor, and editorial board member for various journals.

Anuj Kumar is an Assistant Professor at GLA University, Mathura, India. He received PhD degree in 2017 from Gurukula Kangri University, Haridwar, India. He moved to Beijing University of Chemical Technology, China for his Post Doc research. His research focus is on molecular/M-N-C electrocatalysts for electrocatalysis. He has published more than 125 articles in reputed peer-reviewed journals (like Applied Catalysis B: Environmental, Chemical Engineering Journal, Journal of Materials Chemistry A, Coordination Chemistry Reviews, Chemistry of Materials, Applied Energy etc). He has been awarded with "Best Young Scientist Award 2021" from TAIF. "Young Researcher Award 2020/2021/2022" by InSc and by CEGR. He is serving as Section Editor, Guest editor, and editorial board member for various journals.